Selection of an Appropriate Bedrock for Site Amplification Studies.

Bhavesh Pandey
Indian Institute of Technology Roorkee
Ravi S Jakka (jakkafeq@iitr.ac.in)
Indian Institute of Technology Roorkee

Research Article

Keywords: Site Effects, Bedrock Stiffness, Strong Ground Motion, Amplification, Impedance Contrast

Posted Date: September 17th, 2021

DOI: https://doi.org/10.21203/rs.3.rs-898670/v1

Version of Record: A version of this preprint was published at Natural Hazards on February 25th, 2022.
See the published version at https://doi.org/10.1007/s11069-022-05260-8.

Title: Selection of an appropriate bedrock for site amplification studies.

Authors:

Bhavesh Pandey

Department of Earthquake Engineering, Indian Institute of Technology, Roorkee, Roorkee – 247667. India

Present Address/Affiliation: BT Kumaon Institute of Technology, Dwarahat, Uttarakhand, India.

Email Id: bhawesh.pandey@gmail.com

Ravi S Jakka (Corresponding Author)

Department of Earthquake Engineering, Indian Institute of Technology, Roorkee.

Email Id: rsjakka@gmail.com

Declaration:

Funding: The Ministry of Earth Sciences (MoES), Government of India, for providing financial support for the research (Project Grant Number MoES/P.O.(Seismo)/1(263)/2015)

Conflicts of interest/Competing interests: No conflict of interests

Author's Contributions

Bhavesh Pandey: Conceptualization, Methodology, Software, Investigation, Validation, Writing – Original Draft, Data Curation

Ravi S Jakka: Conceptualization, Methodology, Supervision, Project Administration, funding Acquisition, Writing - Reviewing and Editing

Abstract: The selection of half-space or reference sites significantly influences site amplification studies. However, there are no well-defined guidelines in the literature. Generally, a layer with a local shear wave velocity (V_S) of more than 760 m/s is considered a bedrock/half-space/reference site. This study attempts to formulate a rationale for selecting bedrock stiffness to be used as a half-space/reference site. For this study, $V_{S,30}$ (average shear wave velocity of top 30-meter soil strata from shear wave velocity measurements) and the site's fundamental frequency (obtained from Horizontal to vertical spectral ratio of ambient vibration records) were used as proxies to study the influence of bedrock/half-space and development of a rationale for their selection. This study uses strong-motion data from India's sixty-two strong motion stations and a few from Japan (Kik-Net). The results suggest that considering a site with a shear wave velocity of 760 m/s may not be suitable as a half-space/bedrock for most geomorphological conditions. The results also recognize a pattern that can help in the development of a mathematical model for determining the bedrock for a site using $V_{S,30}$ and its fundamental frequency as a proxy.

Keywords: Site Effects, Bedrock Stiffness, Strong Ground Motion, Amplification, Impedance Contrast

1. Introduction

The influence of local geological and soil conditions on the intensity of ground shaking and earthquake damage has been known for many years. MacMurdo (MacMurdo 1824) noted that "buildings situated on rock site were not by any means so much affected… as those whose foundations did not reach to the bottom of the soil" during the earthquake in Cutch, India, 1819. Later on, damage surveys of several other earthquakes also strengthened the hypothesis that sub-

surface geological conditions can significantly amplify the ground motion. Improvement in technology and the availability of strong-motion recording sensors further helped study and quantify local geology's impact on ground motion. With subsequent developments in the subject, provisions specifically accounting for local site effects were also incorporated by regulatory authorities in their building design codes worldwide.

Local site conditions influence amplitude, frequency content, and duration of strong ground motion. The extent of their influence depends on the subsurface materials' geometry and material properties, site topography, and input motion characteristics (Kramer 1996). The broad categorization of site-effects, as per geological and geotechnical conditions, provide three significant groups, which are *"Effect of Topography", "Effect of Geomorphology", and "Effect of Bedrock Depth and its Stiffness"*. These effects play their role in modifying ground motion; however, the current study's primary focus is the effect of bedrock depth and its stiffness.

The site effects on earthquake motion are widely accepted and incorporated by most modern codal provisions to design structures susceptible to seismic loadings. Typically, these guidelines use a constant amplification factor based on the site class of the respective site. Shear wave velocity of the top 30-meter soil cover ($V_{S,30}$) is the most widely accepted criterion for defining site classes. This classification is solely based on $V_{S,30}$. It ignores soil layers' properties beyond the 30-meters depth, significant impedance contrast before or beyond 30 m depth, and the impedance contrast between bedrock and soil cover. Site classification based on $V_{S,30}$ may cause erroneous estimation of site amplification for the cases with deep soil cover or abrupt stiffness change between soft soil cover and stiff soil layer/bedrock (Bray and Rodríguez-Marek 1997; Dobry et al. 2000; Rodriguez-Marek et al. 2001; Pitilakis 2004; Far et al. 2012; Adhikary et al. 2015; Manandhar et al. 2016). Bray and Rodriguez-Marek (Bray and Rodríguez-Marek 1997)

and Pitilakis *et al*. (Pitilakis 2004) studied the effect of bedrock on-site amplification. These studies proposed alternative site classification schemes with parameters such as depth up to seismic bedrock or Engineering Bedrock (EB), average V_S up to EB, the site's fundamental period, SPT N-values, etc. Bray and Rodriguez-Marek (Bray and Rodríguez-Marek 1997) took a layer with V_S equal to or greater than 760 m/s as EB, and Pitilakis et al. [6] considered 800 m/s EB for their respective classification schemes. In both studies, the NEHRP site classification was considered base classification. These studies proposed sub-classes for NEHRP site classification as per the chosen parameters.

Along with available provisions in various building codes, which help estimate amplification at a particular site using site characteristics, the bedrock's stiffness is also an essential parameter in multiple studies related to seismic hazard assessment. These studies can be broadly grouped into three categories as per the adopted methodology. First is, formulation of regression equations where bedrock characteristics are used as a reference value for amplification function (such as $amplification = f(V_{S,30}, V_{S,ref})$). Secondly, the half-space in shear wave velocity (V_S) profiles is used as theoretical ground response analysis input. Such studies consider the soft soil stratum is resting on a rigid base, i.e., Half-Space extending up to infinity. The third is identifying the possible reference site (nearby hard-rock site from the investigation site) to estimate the amplification function using the Standard Spectral Ratio technique.

Although depth and stiffness of bedrock are essential parameters that influence ground motion, there are no well-defined guidelines available in the literature to incorporate these parameters' effect on the estimation of site amplification. Most of the site amplification studies prefer to use soil layer (or site) having V_S (or $V_{S,30}$) equal to or greater than 760 m/s (NEHRP site class B sites) as bedrock (or reference value).

Steidl et al. (Steidl et al., 1996) explored the importance of correct bedrock for site amplification studies and underlying ambiguity in its selection. However, this ambiguity has not been cleared after the passing of two decades, and more research is required to answer the question raised by Steidl et al. (Steidl et al. 1996). Hence, in this study, an attempt has been made to explore the problem's solution by combining the results of theoretical and experimental methods of site amplification estimation techniques. This study attempts to formulate a rationale for estimating a value that can be used as a Half-space/Reference site (in terms of V_S) for a particular site depending upon proxies such as $V_{S,30}$ and fundamental frequency obtained from Horizontal to Vertical spectral ratio of ambient vibration record. Available data from 62 stations of Indian strong-motion networks (Pandey et al. 2016, 2021)and a few Japanese Kik-Net stations are used for this study.

2. Methodology

Estimation of local site effects is a complicated problem due to several uncertainties. The site amplification estimation problem can be approached by experimental techniques, empirical methods, and theoretical/mathematical modelling. Typically site amplification studies are concerned with two pieces of information, the first is the maximum amplification in ground motion, and the second is the frequency corresponding to maximum amplification. The plot showing amplification amplitude with respect to frequency is known as the transfer function. Several methods are available in the literature which addresses the methodology to estimate the transfer function. These can be broadly divided into theoretical and experimental techniques. The most straightforward method to determine the fundamental frequency of the soil is the use of the average velocity of the soil column, considering it to be fixed at the bottom and free at the top given as $f_{th} = {}^{V_S}/_{4H}$ Where V_S is the average shear wave velocity, and H is the depth of the soil

column. However, this technique can only estimate the fundamental frequency of the soil column (or layer(s)) considered and give no idea regarding the possible amplification at that frequency. Several other methods can provide the amplification for a whole spectrum of frequencies considered. A combination of such theoretical and experimental techniques has been used in the current study, which are Equivalent linear 1-D ground response analysis (GRA), Standard Spectral Ratio (SSR), and Horizontal to Vertical Spectral Ratio (HVSR).

2.1. Equivalent Linear 1-D Ground Response Analysis (Theoretical Technique)

Soil is known to have a non-linear response even at low values of strain. However, consideration of pure non-linear behaviour of soils is difficult as this requires complex constitutive models. This problem can be solved by modifying the linear approach to accommodate the non-linear behaviour of the material. The cyclically loaded soils' non-linear hysteretic stress-strain behaviour is approximated by equivalent linear soil properties such as modulus reduction (G/G_{max}) and damping ratio. Secant shear modulus is calculated as the slope of the line joining the two ends of the hysteretic curve, which is typically taken as equivalent linear shear modulus, G. The damping ratio that produces energy loss equal to the energy loss in a single cycle of the hysteresis loop is considered as equivalent linear damping ratio, ζ for a particular strain in the sample. The dynamic properties, G and ζ, are strain-dependent properties and the linear approach requires that they remain constant for each soil layer. For estimating G and ζ, laboratory tests such as cyclic triaxial test, resonant column test, etc., are used with simple harmonic loading, which has an amplitude equal to the earthquake's peak amplitude motion. In earthquake loading, maximum amplitude occurs only for a few peaks. Hence it can be understood that higher strains will be generated in the case of harmonic loading. To account for this, typically, the earthquake loading strain is characterized by an effective shear strain. The effective strain varies between

50% to 70 % of the harmonic case's maximum shear strain. Most of the time, the effective strain is taken as 65 % of the maximum value. Since values of strain and equivalent linear properties are inter-dependent, the iterative procedure is employed to compute the strain levels. In each iteration, equivalent linear properties corresponding to the strain are calculated to reduce computed value and input error. Once the equivalent linear properties are calculated, they are used for the estimation of the transfer function.

Such analysis can be performed through several available computer programs, such as SHAKE2000, STRATA, DEEPSOIL, etc. An open-source software platform known as STRATA (Kottke et al., 2013) has been used for this study. STRATA is a very user-friendly open-source software to perform 1-D ground response analysis.

The soil strata's layering information was collected from available literature (Pandey et al. 2016, 2021). Similarly, the dynamic properties for the corresponding soil type of each layer are selected from the literature. The detailed soil strata for the sites suggest that most sites are in the Ganga basin, mainly composed of silt and sand. Hence, the Sand average curve proposed by Seed and Idriss (Seed and Idriss 1970) has been used for such sites. Similarly, for sites in the piedmont zone (Tarai region of Uttarakhand), the soil is predominantly composed of gravels after a shallow layer of a mixture of sand and gravels. In such a situation, up to the first few meters, the sand average curve (Seed and Idriss 1970) was used, and for deeper layers, the curve for gravelly soil by Seed et al. (Seed et al. 1986) is used. For sites that have rock strata, the dynamic properties of rock were used that were defined by Schnabel (Schnabel 1973). The sites from the Kik-Net database used in this study also had similar soil types; hence similar dynamic properties were used.

2.2. Experimental Techniques

The most popular and widely used experimental technique to characterize site amplification is the **Standard Spectral Ratio (SSR) technique,** proposed by Borcherdt (Borcherdt 1970). SSR can be defined as the ratio of the Fourier amplitude spectrum of horizontal motion for a soil-site record to a nearby rock-site strong-motion time-history from the same earthquake. The nearby rock site is generally termed as a reference site. Hence, this method is also known as the Reference site technique. This method considers two assumptions: path and source effect for both the stations are the same, and the other is that the reference site station does not have any site effects. The supporting argument for the first assumption is the close distance between the stations compared to the source's distance. The second assumption is that the reference station is selected on a rock outcrop to have minimum site effects. However, it is challenging to find any such site, which is free from any site effects, due to which it becomes tough to locate the reference site (Steidl et al. 1996). The difficulty in finding the reference site is the major drawback of this methodology.

However, a reference site is not required if the surface to downhole spectral ratio is used, considering the downhole record as a reference record. This ratio is also known as Kagami's ratio (Kagami et al. 1982). It was previously believed that such a ratio of surface to bedrock, where the rock site is directly below the surface site and much deeper than the local geological conditions to be studied, would be ideal. However, later studies (Liu et al. 1992; Steidl et al. 1996; Safak 2001) differ from this idea due to remarkably high amplification at particular frequencies in the transfer function estimated using Kagami's approach. Such high amplification values do not correctly compare the effect of site condition on seismic motion recorded at soft soil and rock sites. The said high amplification is caused due to the holes formed at these

frequencies in the ground motion recorded by the downhole sensor. The downhole sensor records reflected waves from the surface and intermediate layers along with the incident waves coming from the source. Therefore, the downhole ground motion record (used as input motion in Kagami's ratio) is the sum of incident waves travelling upwards and reflected waves travelling downwards. The reflected waves contain particular frequencies, depending on the overlying soil layering. The amplitude of these frequencies gets subtracted from the incident motion to be recorded by the downhole sensor. If the downhole sensor had been placed on a free surface, this reduction would not have occurred. The decrease in amplitude of downhole ground motion can be easily corrected by multiplying the ratio by coherence function of input and output, which is given by the following equation;

$$C_{12}^2 = \left|X_{s,b}(f)\right|^2 / (X_{s,s}(f) X_{b,b}(f)) \qquad \text{--------- Eq 1}$$

where, $X_{s,b}(f)$ is defined as Fourier transform of cross-correlation of signals recorded at surface and borehole, $X_{s,s}(f)$ and $X_{b,b}(f)$ is Fourier transform of the autocorrelation of surface and borehole records.

Another famous experimental technique is the **Horizontal to Vertical Spectral Ratio (HVSR)** of ambient vibration (HV_{amb}), which was first introduced by Nogoshi and Igarashi (Nogoshi and Igarashi 1970), and later developed by Nakamura (Nakamura 1989) for estimation of site response. A similar methodology was used by Langston (Langston 1979), using earthquake records to understand the crustal and upper-mantle structure of the earth using teleseismic recordings. Ground motion time history from one station with three channels (two horizontal and one vertical) is sufficient for this technique. This method is also known as the Single station method or Non-reference site technique. This feature makes this methodology very user-friendly

and time-saving, making it very popular among earthquake engineers and seismologists in the last couple of decades.

Besides HVSR of ambient vibration, HVSR of earthquake records (HV_{eq}) is also helpful in estimating site effects. The shape of the site response curve calculated from SSR and HV_{eq} was similar most of the time when the S-wave part of the seismogram was used in several comparative studies (Field and Jacob 1995; Bonilla et al. 1997; Riepl et al. 1998; Triantafyllidis et al. 1999; Parolai et al. 2000, 2001, 2004). Although both methods were consistent in estimating the site's fundamental resonance frequency, their estimated amplification levels differ. For this study, both experimental techniques were used depending upon the availability of data. For Indian sites, HV_{amb} was estimated for all the sites; however, HV_{eq} was calculated for the sites wherever earthquake records are available. Along with Indian sites, few cases from the Kik-Net database were also used to validate the findings from the Indian dataset and fill the gaps where the Indian dataset is not available. Kik-Net database has earthquake records from the surface and downhole sensors at each site location. Hence, for these sites, SSR and HVSR were used to estimate the experimental site amplification function. For SSR, Kagami's approach (Kagami et al. 1982) is used along with correction using coherence function as discussed earlier. For $HV_{eq,}$ low-intensity earthquake records were used for the estimation of transfer functions. For the estimation of HVSR and SSR, the resultant horizontal ground motion is used given as;

$$Acc_{Hor} = EW + iNS \qquad \text{Eq 2}$$

Acc_{Hor} is a resultant horizontal record, EW is the East-West component of the record, and NS is the North-South component. Furthermore, the Konno-Omachi smoothing function (Konno and Ohmachi 1998), which is defined as $\left(\frac{\sin(blog10(f/f_c))}{blog10(f/f_c)}\right)^4$ used for smoothing. In this function, f denotes frequency, f_c is central frequency, and b is bandwidth. This smoothing function ensures

a constant number of points at low and high frequencies. Hence, it is mainly preferred for frequency analysis where the frequency axis is preferably in a logarithmic scale. A bi-directional Butterworth low-cut filter was applied at the cutoff frequency of 0.25 Hz for both analyses (Boore 2005; Converse and Brady 1992).

2.3. Site classification and analysis

The sites used in this study belong to NEHRP site classes C and D. For this study, these sites were further divided into six groups in terms of $V_{S,30}$ and depth of engineering bedrock (EB) (EB is considered as the first layer which has V_S greater than 760 m/s) as follows;

- Group 1a (G1a): $V_{S,30}$ > 360 m/s and depth of EB < 50m
- Group 1b (G1b): $V_{S,30}$ > 360 m/s and depth of EB between 50 and 100 m
- Group 1c (G1c): $V_{S,30}$ > 360 m/s and depth of EB > 100m
- Group 2a (G2a): $V_{S,30}$ < 360 m/s and depth of EB < 50m
- Group 2b (G2b): $V_{S,30}$ < 360 m/s and depth of EB between 50 and 100 m
- Group 2c (G2c): $V_{S,30}$ < 360 m/s and depth of EB > 100 m

The details of sites belonging to the Indian strong motion network and Japanese network are presented in Table 1 and Table 2.

V_S profiles of the Indian sites are obtained from the available literature (Pandey et al. 2016, 2021), and Kik-Net sites are obtained from the webpage http://www.kyoshin.bosai.go.jp, which were used for ground response analysis. Multiple ground response analysis was performed for each site using V_S profiles up to different depths extracted from the original V_S profile (Figure 1) to study the bedrock effect. The transfer function for each such V_S profile is estimated between surface and bedrock (as outcrop).

For most cases, the half-space of all the extracted V_S profiles for a particular site has V_S equal to or more than EB. For sites where a significant impedance contrast is encountered at a shallower depth, layers having V_S less than 760 m/s were also considered half-space (Figure 1) for GRA. For GRA, both horizontal components (East-West and North-South) for all the ground motions recorded at the sites are used as input motion at the top of the ground surface. All the input motions are then deconvoluted to the top of half-space. Output motion from ground response analysis is extracted as outcrop motion rather than within motion to estimate the transfer function at the top of half-space. The median of all the transfer functions obtained from different input motions (available for that specific site) for each V_S profile was used for the comparative analysis.

Considering Figure 1 as an example, five V_S profiles were extracted from the initial V_S profile by curtailing the initial V_S profile up to a certain depth. The depth selection for the first V_S profile is based on the original V_S profile's visual inspection to determine the significant impedance contrast or layer having V_S equal to or more than 760 m/s. The layer below the selected depth is considered as half-space for that particular V_S profile. After the first V_S profile is obtained, the next layer below the first V_S profile's half-space is regarded as half-space for the second V_S profile with extended depth to the top of the new half-space. Similarly, continuing the process and considering the depth and half-space by considering the last V_S profile's immediate deeper layer, remaining V_S profiles were extracted. Hence, five V_S profiles were used having half-space with $V_{S\text{-}HS}$ (shear wave velocity of half-space) equal to 675 m/s, 725 m/s, 775 m/s, 1000 m/s, and 1250 m/s, for GRA providing five transfer functions for this particular example. These transfer functions were further compared with transfer functions obtained from HV_{amb} and HV_{eq}. With the comparison of different transfer functions, it can be seen that the peak frequency lying between 7

to 10 Hz can also be derived from the first V_S profile, which rests over the soil layer having V_S equal to 675 m/s. GRA with more in-depth layers contributes to the increase in amplification amplitude, suggesting that a profile with this layer (V_S = 675 m/s) as half-space is not suitable for estimating transfer function. The reason for this conclusion is, although this profile is good enough to estimate the natural frequency of the site, it cannot estimate the amplification amplitude accurately. Similar reasoning has been employed for all other sites to study the effect of different layers as half-space to evaluate transfer function.

For sites where no earthquake record was available, "CHICHI AFTERSHOCK 09/20/99 1803, TCU138, W, (CWB)" was used after multiplying by a scaling factor of 0.2. The scaling was done to reduce the intensity of motion so that non-linear site effects may be avoided. These records were of low intensity for sites wherever earthquake records were available; hence, no scaling was required.

Thus, the transfer functions were compared with HV_{eq} (wherever available) and HV_{amb} to determine which V_S profile first achieves the fundamental frequency for Indian sites. Similarly, for Kik-Net sites transfer function from GRA was compared with the transfer function obtained from HV_{eq} and SSR (in place of HV_{amb}).

3. Results

The results of the study are discussed in groups, as described earlier. For ease of understanding, G1a and G2c groups, which have the maximum number of sites and variability, are presented in multiple figures as per their geographical locations. Further, few sites are discussed in more detail to understand the analysis process and wherever unique interpretations can be made. This

section has been further divided into subsections as per the groups for ease of understanding of the results and better readability.

3.1. Group G1a sites ($V_{S,30}$ > 360 m/s & D_{EB} < 50 m)

G1a sites are situated in two different terrain and geographical regions, the first are located in Delhi, and the other are located in the Himalayan region of Uttarakhand. Delhi region's sites can be divided into two categories, one lying on Delhi Ridge, the extension of the Aravalli range. Another set of sites are located on the flood plains of the Yamuna river. The sites situated on Delhi ridge have shallow weathered rock structures from the ground surface itself, and these sites fall under group G1a. All the sites located in the Himalayan region of Uttarakhand fall under the G1a group. Due to this reason, the results are presented separately for Delhi and Himalayan sites.

Sites in Delhi Region: Geographically, all the G1a sites used in this study are located in Delhi and Uttarakhand's Himalayan region. The results of G1a sites located in Delhi are presented in Figure 2. Considering the results of IGNOU, it can be inferred that the frequency corresponding to the highest amplification is equal to 16.84 Hz. This frequency can be seen in all the transfer functions obtained from GRA, starting from the V_S profile with a depth of only 20 meters and the half-space of 650 m/s. However, the amplification was very low for the profile resting over the layer having V_S equal to 650 m/s and have a single peak compared to the transfer function obtained from GRA of other V_S profiles. Hence, it cannot be considered an appropriate half-space to estimate the transfer function. There is no significant change in transfer functions at the frequency for all other V_S profiles with $V_{S,HS}$ (shear wave velocity of half-space for the considered profile) greater than 850 m/s and the D_{HS} (half-space depth for the considered profile) 40 meters corresponding to maximum amplification. Maximum amplification is also observed in the 12.2 – 16.8 Hz frequency band in the transfer function obtained from HV_{amb} and HV_{eq}. Both

317 the frequencies correspond to two neighbouring maxima in transfer functions of GRA. The peak
318 amplitude at the frequency band of 3.5 – 4 Hz was observed to increase for more in-depth V_S
319 profiles with layers beyond the V_S layer equal to 850 m/s. A similar maximum at 3.5 Hz is also
320 observed in HV_{amb} and HV_{eq}. However, these profiles do not cause any significant change in the
321 frequency of most peaks observed for the V_S profile, which has $V_{S,HS}$ of 850m/s, but amplification
322 was observed to increase by more than 15%. Hence, this layer (850 m/s) cannot be an
323 appropriate half-space. With this criterion (that there should be a minor change in amplification
324 and frequency shift while using deeper profiles), a layer with V_S of 1000 m/s qualifies as an
325 appropriate half-space for performing GRA for this site.

326 A trend similar to IGNOU is observed for ANDC (Figure 2) site, where the frequency with the
327 highest amplification was observed at 13.5 Hz. This trend is evident from all the transfer
328 functions, which have a half-space of V_S of more than 1050 m/s. HV_{amb} and HV_{eq} also show
329 maximum close to this frequency. However, the first significant maximum in HV_{amb} and HV_{eq}
330 occurs between 3 – 4.4 Hz. This maximum matches the maximum observed in the transfer
331 function estimated by GRA for the profile with $V_{S,HS}$ equal to 2000 m/s at a depth of 342 meters.
332 It can be observed that maximum amplification and its corresponding frequency for this site can
333 be easily calculated with a profile with a depth of 122 meters and $V_{S,HS}$ of 1400 m/s using GRA.
334 However, this profile is not capable of capturing the amplification below 6 Hz of frequency.

335 Similarly, for the VCD site (Figure 2), fundamental frequency from HV_{amb} and HV_{eq} was
336 observed at the frequency band of 4.3 to 4.8 Hz. For VCD, an appropriate half-space or reference
337 site should be the site with $Vs_{,HS}$ more than 1700 m/s. For IMD (Figure 2), fundamental
338 frequencies obtained from HV_{amb} and HV_{eq} were observed in the frequency band of 8.5 – 9 Hz. A
339 similar fundamental frequency was observed for transfer functions obtained from GRA of V_S

profiles with varying half-space from $V_{S,HS}$ of 750 m/s to 1250 m/s having respective D_{HS} of 10 meters to 120 meters. For this site, no significant amplification was observed for lower frequencies with an increase in depth and *Vs* of half-space, similar to the observation of IGNOU results. The fundamental frequency obtained from the analyses is identical to the fundamental frequency obtained from GRA, equal to 8.75 Hz. Therefore, it can be concluded that for GRA, a profile up to the layer which has V_S similar to 1050 m/s is sufficient for this site. For JNU (Figure 2), profiles studied for the analysis have $V_{S,HS}$ from 800 m/s to 1400 m/s, and D_{HS} of 22 meters to 97 meters. Using these profiles, the transfer function obtained from GRA shows maximum amplification in the 12.5 – 13 Hz frequency band. Significant amplification can also be observed in the transfer function obtained from HV_{amb} at this frequency. The change observed in amplification at this frequency was insignificant for profiles with deeper layers beyond 1025 m/s. However, few local maxima can be observed at lower frequencies for more in-depth profiles. The lowest frequency, for which a maximum is observed, is 3.5 Hz which corresponds to the profile going up to $V_{S,HS}$ of 1200 m/s. HV_{amb} for this site also shows maximum amplification at 3.5 Hz. Therefore, an inference can be made from these results that a profile of 1200 m/s or more would be required for studying the amplification at this site.

Sites in the Himalayan region of Uttarakhand: Among the 62 sites, BAG (Figure 3) has the highest $V_{S,30,}$ equal to 736 m/s. The fundamental frequency for BAG observed from the result of HV_{amb} was around 10 Hz. The transfer function obtained from GRA using V_S profile with a half-space of 2200 m/s at a depth of 148 meters shows maximum amplification at approximately 10 Hz. For all V_S profiles shallower than 148 meters, the maximum amplification in GRA's transfer functions occurs at a much higher frequency of around 20 Hz. The comparison of various transfer functions of CKT (Figure 4), which has $V_{S,30}$ equal to 622 m/s and a fundamental

363 frequency between 2 – 3 Hz from HVSRs, shows a similarity with the results of IGNOU, VCD,
364 ANDC sites. The transfer function estimated (using GRA) from the profile up to 2100 m/s
365 captured the lowest frequency peak, which was the highest in HV_{amb} at around 3 Hz. However,
366 the GRA's transfer function has higher amplitudes at maxima occurring at frequencies greater
367 than 3 Hz. There could be several reasons for such behaviour. One reason for higher frequency
368 from GRA is amplification dominance due to shallow layers' impedance contrasts. The second
369 reason is the presence of topographical effects, which caused lower frequency in HV_{amb} and
370 HV_{eq}, as this site is located at the hilltop. However, this study's focus is only to study the change
371 in transfer function with respect to different half-space conditions; hence all other aspects are
372 ignored if found only in few cases as the exception. A similar phenomenon has been observed
373 for other sites located at the hilltop discussed later in the text. The maximum amplification for
374 CKT calculated from GRA occurs at 20 Hz for all the transfer functions with $V_{S,HS}$ greater than
375 1000 m/s and a depth of 21 m. CHP (Figure 3), which has a fundamental frequency estimated
376 from HVSRs around 6.2 Hz, shows similar IMD trends with maximum amplification from GRA
377 at 6.2 Hz. For CHP, all the transfer functions from GRA, obtained from various profiles with
378 $V_{S,HS}$ greater than 760 m/s, show maximum amplification at around 6.2 - 6.5 Hz. These transfer
379 functions suggest a half-space or reference layer of 760 m/s or more can be sufficient to estimate
380 the fundamental frequency of this site, but that would not estimate the amplification correctly.
381 This conclusion arises from the fact that amplification increases in each transfer function. Hence,
382 observations from transfer functions from deeper profiles suggest that a half-space of 1600 m/s
383 would be necessary to estimate amplification. For DNLT (Figure 4), which has $V_{S,30}$ equal to 418
384 m/s and fundamental frequency equal to 3 Hz from HV_{amb}, maximum amplification from GRA
385 occurs at 7.5 Hz. This frequency of 7.5 Hz first occurs for a half-space of 935 m/s and remains

386 constant for a deeper half-space or reference layer with higher Vs. Similar to several analysis
387 results of the sites presented earlier, lower frequency amplification is seen with deeper layers as
388 half-space, but the maximum amplification remains at 7.5 Hz. The local maximum at 2.9 Hz
389 appears with the introduction of half-space having V_S equal to 1325 m/s. Furthermore, any layers
390 below this layer do not contribute much to either amplification or frequency. These observations
391 suggest that a half-space of 1325 m/s or more would be sufficient to estimate site effects at
392 DNLT. DMKT has a $V_{S,30}$ of 577 m/s and fundamental frequency from HV_{amb} equal to 5.4 Hz.
393 For this site, similar to CHP, maximum amplification occurs at the frequency of 5.4 Hz. These
394 results show that this frequency can be estimated with a half-space of 1000 m/s at a depth of 22
395 m. Still, the amplification evaluated by this profile increases significantly for the deeper profiles
396 with a stiffer base. Considering all the cases studied, the profiles with half-space deeper than
397 1600 m/s at a depth of 104 meters does not contribute much to amplification. Hence, it can be
398 said conveniently that deeper profiles would not be required to estimate a transfer function for
399 this site, and 1600 m/s can serve as a reliable half-space for the GRA. For JMTH (Figure 4)
400 having $V_{S,30}$ of 522 m/s, two peaks were observed in HV_{amb} at a frequency of 1.1 Hz and another
401 at 6.9 Hz. The HV_{amb} of JMTH suggests that a shallow layer at 24 meters of depth with Vs of 900
402 m/s significantly contributes to the HV_{amb}. However, the maximum amplitude from GRA occurs
403 at a much higher frequency corresponding to the impedance contrast caused by the layer of 510
404 m/s located at a depth of 6 m. While performing GRA with layers underneath 900 m/s layer as
405 half-space, the 1.1 Hz frequency is estimated with the half-space lying at 217 meters depth and
406 Vs of 1650 m/s.

407 For KAP (Figure 3) with $V_{S,30}$ of 440 m/s and $f_{0,hv}$ at 4 Hz half-space of 1050 m/s at a depth of 45
408 meters provides satisfactory results. Similar to JMTH, LNSD (Figure 4) also has two significant

409 peaks in HV_{amb} at 3 Hz and 12.3 Hz. In this case, a half-space of 1400 m/s at a depth of 130
410 meters is good enough for any site amplification study. For MUN (Figure 3), which has $V_{S,30}$
411 equal to 582 m/s and $f_{0,hv}$ at 11.7 Hz, a profile with half-space at 9 meters depth with Vs of 700
412 m/s can estimate the fundamental frequency, but it cannot account for the amplification at lower
413 frequency peaks in HV_{amb}. Hence, considering GRA results using all possible half-space
414 situations, the layer with 1400 m/s at a depth of 165 meters was found to be appropriate. For
415 NTL (Figure 3), which has a lower $V_{S,30}$ of 412 m/s and $f_{0,hv}$ of 3.625 Hz, no significant
416 amplification is observed for the soil profiles having half-space deeper than 900 m/s soil/rock
417 layer, which is located at a depth of 43 meters. For VKN and TNKP, sites located in the Bhabhar
418 region of Uttarakhand are known for deep deposits of boulders mixed sand, an HS with $V_{S,HS}$
419 more than 1250 m/s is found to be sufficient.

420 Summarising the results for sites in the G1a group (Table 3), which have $V_{S,30}$ greater than 360
421 m/s and EB less than 50 meters, the observations and inferences are further regrouped as per the
422 site's $V_{S,30}$ and fundamental frequency. The sites are further divided into sub-classes as per the
423 $V_{S,30}$, $f_{0,hv}$, and recommendations for bedrock. For the sites with $V_{S,30}$ greater than 600 m/s (sub-
424 class C1), the half-space or reference site must be greater than 2000 m/s. From the available
425 database of Indian sites, such half-space is mostly observed at a depth of more than 100 meters.
426 Similarly, for sites with $V_{S,30}$ between 500 to 600 m/s and the first peak frequency of HV_{amb} more
427 than or close to 5 Hz (sub-class C2), a half-space or reference site having V_S equal to or more
428 than1500 m/s can be used. For sites with $V_{S,30}$ between 400 to 500 m/s and first peak frequency
429 at more than 3 Hz (sub-class C3), a half-space or reference site with local Vs of 1000 – 1200 m/s
430 can also be used. However, if the site has the first maximum at a frequency around 1 Hz (sub-

class C4), then half-space should be greater than 1500 m/s for all sites with $V_{S,30}$ greater than 400 m/s.

3.2. Group G1b sites ($V_{S,30}$ > 360 m/s & 50 m < D_{EB} < 100 m)

Only two sites (NSIT and BKT) were available in group G1b (Figure 6). The results of G1b sites can only provide an understanding regarding sites with $V_{S,30}$ around 400 m/s due to the non-availability of sites. However, these results help reaffirm the earlier inferences for cases with $V_{S,30}$ around 400 m/s. These inferences suggest the requirement of half-space with V_S equal to 1500 m/s if the $f_{0,hv}$ is around 1 Hz (sub-class C4) and a half-space with V_S equal to 1000 – 1200 m/s if the fundamental frequency is more than 3 Hz (sub-class C3).

3.3. Group G1c sites ($V_{S,30}$ > 360 m/s & D_{EB} > 100 m)

For G1c sites (Figure 7), a half-space with local *Vs* of 1000 – 1200 m/s can provide good results with the condition that this would be valid for sites having $V_{S,30}$ between 360 – 400 m/s due to the non-availability of sites having $V_{S,30}$ above 400 m/s. Again, these results reaffirm the earlier inferences for sites with $V_{S,30}$ around 400 m/s and $f_{0,hv}$ ~ 1 Hz (sub-class C4). Considering the results from G1a, G1b, and G1c sites, which have $V_{S,30}$ values close to 400 m/s, it can be concluded that the depth of EB (engineering bedrock, i.e. the first layer with V_S equal to 760 m/s and more) does not play a significant role in the site amplification of sites belonging to group 1. Hence, the depth of engineering bedrock is not an essential site parameter for these sites. However, the $f_{0,hv}$ seems to correlate much better with different amplification functions and site properties. This behaviour is because EB does not provide the necessary impedance contrast for these sites, which causes the amplification at a particular frequency. Much deeper layers are responsible for such amplification shifting the peak to a lower frequency. Hence, proper care

must be taken in such cases while estimating site amplification using GRA or SSR where half-space or reference site's stiffness plays an important role.

3.4. Group G2a sites ($V_{S,30}$ < 360 m/s & D_{EB} < 50 m)

As discussed earlier, due to the unavailability of sites in the G2a group, four sites were selected from the Kik-Net database to see the effect of bedrock depth in this category. The details of these sites are presented in Table 2. While using Kik-Net sites, SSR (Kagami's ratio) is used in the place of HV_{amb}. $V_{S,30}$ of the selected sites are equal to 238 m/s (AOMH05), 261 m/s (AOMH09), 243 m/s (KKWH11), and 355 m/s (KKWH13). All these sites have a fundamental frequency at around 2 Hz except KKWH13, which shows fundamental frequency estimated using HV_{eq} and SSR at around 5 Hz. In the case of KKWH13 (Figure 12), it seems that the top layer, which has V_S equal to 230 m/s and depth equal to 8 meters, is governing the response. The fundamental frequency calculated for this layer is equal to 7.2 Hz ($f = V_S/4H$), which is similar to the frequency obtained by HV_{eq} and SSR. The fundamental frequency from the transfer function estimated using GRA is around 3 Hz, similar to the fundamental theoretical frequency calculated using $f = V_S/4H$ (3.25 Hz) for 24 meters deep profile. No significant change was observed in fundamental frequency in the transfer functions estimated using GRA for profiles with layers beyond 800 m/s. Amplification seems to increase continuously for profiles having deeper and stiffer HS, due to which 800 m/s may not be a good HS for estimation of amplification even though fundamental frequency can be accurately estimated using such profile. Similarly, for AOMH05 (Figure 12), a dominant peak is observed next to the first peak, which seems to be representing the topmost layer of *Vs* equal to 80 m/s at depth 4 meters. This peak was found to be present in the transfer functions obtained from all three methods. All these results suggest an HS

or reference site of V_S more than 1000 - 1200 m/s is a must for G2a sites, even if they have lower $V_{S,30}$ values. These sites can be classified as sub-class D1, as presented in Table 3.

3.5. Group G2b sites ($V_{S,30}$ < 360 m/s & 50 m < D_{EB} < 100 m)

All the G2b group sites fall in the band of $V_{S,30}$ between 330 – 360 m/s with not many layers below EB in the available shear wave velocity profiles. For GOPE (Figure 8), the fundamental frequency obtained from HV_{eq} is lower than all other transfer functions. The lower frequency estimated from strong-motion records could be due to the topographic effects as GOPE is located on a hilltop. This inference is similar to the observations made from the results of other sites located on the hilltop and discussed earlier. As the topographic effects are not the objective of this study hence for such cases, only HV_{amb} is considered for the analysis and conclusions. Other than GOPE, all other sites in this group do not have such anomalies. If the HV_{eq} for GOPE is not considered and further compared with all other five sites, it can be quickly concluded that a half-space of 1000 m/s or more is necessary for depicting the correct transfer functions for these sites. The depth of half-space will vary with the fundamental frequency of HV_{amb}. For sites with higher fundamental frequency, as obtained for ZHC (Figure 8), this depth could be less than 100 meters. If the first peak frequency is below 2 Hz, this layer will occur at a depth of more than 100 meters. These inferences are similar to the earlier conclusions made from sites with $V_{S,30}$ around 400 m/s that the $f_{0,hv}$ of the site could be a more useful parameter than the depth of EB.

3.6. Group G2c sites ($V_{S,30}$ < 360 m/s & D_{EB} > 100 m)

Figure 9-11 shows the results of sites in G2c arranged as per their geographical location to ease understanding and legibility. Most of the sites in this group have fundamental frequency ~ 1 Hz and $V_{S,30}$ between 200 – 350 m/s. All these sites lie in the Ganga basin area and have deep

alluvial deposits, mainly sandy soil. Four sites viz., SCRG, DTU (Figure 9, c), KSPR (Figure 10), GHZ (Figure 11) have frequency less than 1 Hz, even though the $V_{S,30}$ for these sites is in the range of 282 (KSPR) to 346 m/s (SCRG). The results for these sites suggest that an HS with $V_{S,HS}$ equal or greater than 1000 m/s at a depth of more than 100 meters (if considering as HS) would be required for good results. Other than these sites, which have $V_{S,30}$ greater than 300 m/s must have a half-space of 800 – 1000 m/s. Similarly, for sites with $V_{S,30}$ between 250 to 300 m/s, a half-space of 700 – 800 m/s may be sufficient to get a transfer function that can define the site conditions. In some cases with very low $V_{S,30,}$ such as NJBD ($V_{S,30}$ = 207 m/s), a half-space of 600 m/s was found to be sufficient. However, it is recommended to at least use a half-space with a shear wave velocity equal to 760 m/s. This inference cannot be revalidated as no more sites are available with such a low $V_{S,30}$. The deductions made from these results are presented in Table 3 concisely, which can also be used as recommendations for the required half-space/reference site for different site conditions.

3.7. Crucial observations and inferences

From the various examples and summary presented in Table 3 for sites having $V_{S,30}$ between 300 - 400 m/s, it can be inferred that a softer half-space is good enough for sites with high fundamental (sub-class C3 and D1) frequency in comparison to sites with lower fundamental frequency (sub-class C4 and D2). This is because the sites with a similar average V_S but lower fundamental frequency indicate the deeper layer's ($f = V_S/4H$) involvement in seismic response. For example, for a site in sub-class C3, the impedance contrast responsible for the amplification would be at a depth of around 40 m or lesser (using $f = V_S/4H$). In contrast, for a sub-class C4 site, this depth could be more than 100 m. While, for sites having a higher fundamental frequency and similar average V_S, shallower depths only contribute to the site's transfer function.

For example, for a site in sub-class C3, the impedance contrast responsible for the amplification would be at a depth of around 40 m or lesser (using $f = V_S/4H$). In contrast, for a sub-class C4 site, this depth could be more than 100 m. Similarly, comparing sub-class D1 and D2, the corresponding approximate depths would be 40 m or less for sub-class D1 and 75 m or more for sub-class D2. It is a well-known fact that, typically, soil stiffness increases with depth due to an increase in the overburden. Therefore lower fundamental frequency sites (in other words, the sites for which amplification function is affected by deeper layers) would require stiffer half-space/reference site for estimation of the transfer function, considering $V_{S,30}$ to be the same for these sites.

4. Validation using Kik-Net database

The results and inferences discussed earlier were further validated using a few additional sites from the Kik-Net database. The primary objective of this section is to perform a similar analysis (SSR, HV_{eq}, and GRA) on these sites and check whether similar inferences can be made or not. Another essential objective is to demonstrate a methodology to use the guidelines in Table 3 for achieving a shear wave velocity profile for the site, which can be used for seismic hazard assessment studies. The profiles thus created are further used for estimation of transfer functions using GRA (GRA-th henceforth). These transfer functions were further compared with the transfer function obtained by SSR, HV_{eq}, and GRA to check the usability of these profiles.

The selected sites for this analysis were found to be in groups G2b and G2c (Table 2). In the G2b group, for sites MYGH05 and NMRH02 (Figure 13), the peak frequency seems to be guided by the very soft top layer (Vs = 120 m/s and thickness = 2 meters for MYGH05 and Vs = 110 m/s and thickness = 4 meters for NMRH02). The effect of the top layer is evident in the

542 transfer functions produced by all three methods (SSR, HV_{eq}, and GRA). Although the impact of
543 the top layer is significant in these cases, the transfer function cannot rely only on the top layer,
544 which causes amplification at high frequency. The lower frequency peaks in HV_{eq} can be
545 attributed to the impedance contrast at deeper layers. It is a well-established fact that the HVSR
546 curve shows peaks at frequencies where significant impedance contrast arises (Castellaro 2016).
547 However, SSR and GRA results demonstrate that the peak amplification is the effect of
548 shallower layers only. Hence, the study of the transfer function at peak frequency seems
549 sufficient. Considering the results of both sites, it can be said that HS of 1000 m/s or more could
550 be good enough for such sites. A similar conclusion was drawn earlier from Figure 8, which
551 shows results from Indian sites. The analysis of transfer functions obtained for FKIH04 (Figure
552 14), which has $V_{S,30}$ = 300 m/s, slightly deviates from this conclusion. The deviation can be
553 explained by considering a sudden and huge change in the stiffness/V_S of the layer (order of more
554 than twice) at a depth of 98 meters which seems to be guiding the amplification. Typically, such
555 changes occur in top layers of the soil strata that have softer soil layers. Hence, most of the time,
556 those layers govern the peak frequency of the transfer function.

557 The Indian sites used for this study in the G2c group have a fundamental frequency ~ 1 Hz, but
558 the sites considered from the Kik-Net database have a fundamental frequency greater than 2 Hz.
559 Due to this, the results of G2c sites from the Kik-Net database help to explore the involvement of
560 sharp impedance contrast at shallower depths. Two sites are considered in this group from the
561 Kik-Net database to evaluate the effects of such sharp contrast. From GRA transfer functions, it
562 can be seen that the peak frequency can be easily estimated using the first sharp impedance
563 contrast. Just using that layer as half-space cannot provide a reasonable estimate of amplification
564 that can be seen for site AICH23. For AICH23, a profile with a half-space of V_S equal to 540 m/s

565 at a depth of 30 meters provides a reasonable estimation of the peak frequency and subsequent
566 frequencies. Still, the amplitude increases as the deeper layers are introduced as HS and their
567 corresponding depth in GRA. In this case, the HS of 1200 m/s or more seems necessary;
568 otherwise, the estimate of amplification may go wrong. Similarly, KNGH22 has a broad plateau
569 type of amplification function ranging from 1.8 Hz to 2.8 Hz. Considering the median value of
570 the plateau, i.e. ~2.2 Hz, similar conclusions can be drawn for this site as well.

571 Additionally, another analysis has also been performed for these five sites to check the
572 effectiveness of the recommendations made in Table 3. For this analysis, a theoretical shear
573 wave velocity profile was created for each site as per the recommendation. The transfer function
574 was estimated for each case by equivalent linear ground response analysis (shown as GRA-th in
575 figures 13 and 14). The theoretical profile is created using the following steps,

576 • The shear wave velocity profile of the top 30 meters is extracted from available data.
577 • The last layer of the 30 meters profile is extended up to a certain depth. The depth can be
578 calculated by using the peak frequency obtained from *HVeq* (or *HVamb* if available) and
579 the relation between frequency and average shear wave velocity of the soil strata given
580 as;

581 $$f_0 = V_S/(4 * h)$$

582 • After the depth is obtained from the last step, half-space is provided as per the
583 recommendation of Table 4.

584 For example, consider FKIH04, which has a single layer of 300 m/s shear wave velocity up to 30
585 meters in depth. The same layer has been extended up to 52 meters depth corresponding to 1.4
586 Hz frequency obtained from *HVeq*. The half-space of 1000 m/s shear wave velocity is provided
587 below 52 meters as per the recommendation of Table 4. GRA has been performed for the profile

thus obtained to estimate the transfer function between surface and half-space as an outcrop. The transfer function, thus obtained, is compared with other transfer functions obtained from different methods, as discussed earlier. The results thus obtained are presented in Figures 13 (for G2b sites) and 14 (For G2c sites). The comparison of GRA-th with other transfer functions shows agreement in frequency and amplitudes of the transfer function. For NMRH02, few lower frequency peaks are also evident in *HVeq*. These lower frequency peaks may confuse the user regarding which frequency must be used to develop the hybrid profile. To study these lower frequency peaks in *HVeq* of NMRH02, another GRA-th analysis is performed with the half-space of 1000 m/s and the depth of 202 meters (corresponding to 0.5 Hz) considering a significant peak at the frequency in *HVeq*. This site's available shear wave velocity profile is only up to 94 meters in depth in the Kik-Net database. This peak could be the reason for some significant impedance contrast at deeper layers. As per the results discussed in the earlier section, the half-space used for the deeper profile must have been stiffer; however, due to the non-availability of any such recommendation, 1000 m/s is considered. By studying the results of both sites (MYGH05 and NMRH02), it can be said that HS of 1000 m/s or more is a good approximation of the half-space at an appropriate depth (as per peak frequency) for GRA. Furthermore, for site FKIH04, the amplification of the theoretical transfer function was much lower than the transfer function obtained for the actual profile. This is due to the sharp impedance contrast at 98 meters depth, where the bottom layer's stiffness gets doubled compared to the top layer (from 940 m/s to 2300 m/s). Typically such sharp impedance contrast occurs at the shallower depths with softer soil deposits. Similarly, the hybrid profiles are also sufficient to capture the effect of amplification at peak frequency.

610 This analysis further strengthens the usability and advantage of using such hybrid profiles, which
611 can be generated using $V_{S,30}$ from the actual testing results, depth calculation with the help of
612 fundamental frequency obtained from HVSR, and half-space from the study. These
613 recommendations can also be used as a reference value in regression analysis for amplification
614 studies.

615 ## 5. Summary and Conclusions

616 The study's objective is to understand the effect of bedrock stiffness and its location on the site
617 amplification. To achieve the said objective, site amplification functions were calculated using
618 shear wave velocity profiles considering half-space at different depths using theoretical Ground
619 response analysis (GRA). These amplification functions were compared with transfer functions
620 estimated using ambient noise and earthquake records. Sixty-two sites having detailed site
621 characterization and earthquake records from the Indian dataset were used in this study. The sites
622 used in this study primarily belong to NEHRP site classes C and D. These sites were further
623 divided into six subgroups based on their $V_{S,30}$ and engineering bedrock (EB) depth. Conclusions
624 drawn from this study are summarised below:

625 ➢ This study suggests that the fundamental frequency response of any site depends only upon
626 the particular depth of soil cover, which may or may not be extending up to the top of
627 soft/hard rock.

628 ➢ Outcomes of the study clearly show that layers below a certain depth do not significantly
629 influence the transfer function in soft soil sites (i.e. site class D). However, in many
630 instances, this depth is found to be up to the Engineering Bedrock (EB).

631 ➢ For Site Class C, it is found that considering profile only up to engineering bedrock may not
632 be sufficient.

- For shallow soil sites (i.e. sites having higher fundamental frequency) belonging to NEHRP site class C, deeper layers below EB also significantly contribute to the transfer function. Hence, half-space must be chosen with care to avoid any error in GRA results for such sites.
- Even for site class C, the fundamental frequency is not affected by the deeper layers after a certain profile depth, although this depth is beyond EB.
- However, the amplitude of the fundamental frequency peak is slightly affected by the deeper layers. The presence of deeper layers causes a slight increase in amplification at peak frequency and a few smaller peaks at lower frequencies than peak frequency.
- These results also emphasize the importance of depth and stiffness of bedrock/half-space in site classification apart from $V_{S,30}$, which is not a part of any site classification scheme. It has been conclusively shown that the peak frequency of HV_{amb} can be used as a proxy for incorporating the depth of bedrock.

A new approach has also been suggested to select an appropriate half-space for sites with shallow profiles only up to the top 30 meters. The proposed method offers bedrock stiffness and where it should be provided for different site classes. The appropriate depth of the half-space can be evaluated based on the available profile fundamental frequency, as explained in the validation section (Section 4). The stiffness of a half-space is to be selected based on the $V_{S,30}$ and fundamental frequency (Table 3). The proposed method is also verified using the Kik-Net database. The proposed method is proved to be very useful for obtaining reliable site amplification using theoretical ground response analysis. Further, the recommendations can also be used to select appropriate reference site stiffness for reference site techniques and regression analysis to develop site amplification, prediction models.

These results and recommendations can be further extended to other site classes, with a larger dataset covering other NEHRP site classes. Such a study would also help to review the effectiveness of $V_{S,30}$ & the fundamental frequency of the site as proxy variables for site amplification and development of regression models.

6. Acknowledgement

The authors wish to thank the Ministry of Earth Sciences (MoES), Government of India, for providing financial support for the research (Project Grant Number MoES/P.O.(Seismo)/1(263)/2015). We are also thankful to the Head of Department, Department of Earthquake Engineering, and the laboratory staff for their help in testing and fieldwork.

7. References

Adhikary S, Singh Y, Lang DH, Kumar R (2015) Effect Of Soil On Seismic Performance And Vulnerability Of RC Frame Buildings. *In: SECED 2015 Conference: Earthquake Risk and Engineering towards a Resilient World* 9-10. Cambridge UK

Bonilla LF, Steidl JH, Lindley GT, et al. (1997) Site amplification in the San Ferdinando Valley, California: variability of site effect estimation using S-wave, coda, and H/V methods. *Bull Seism Soc Am* 87:710–730

Boore, DM (2005) On Pads and Filters: Processing Strong-Motion Data. *Bull Seism Soc Am* 95:745–750, https://doi.org/10.1785/0120040160

Borcherdt RD (1970) Effects of local geology on ground motion near San Francisco Bay. *Bull Seism Soc Am* 60:29–61

Bray JD, Rodríguez-Marek A (1997) Geotechnical site categories. *In: Proceedings of the First PEER-PG&E Workshop on Seismic Reliability of Utility Lifelines*. San Fransisco, CA

Castellaro S (2016) The complementarity of H/V and dispersion curves. *Geophysics* 81:T323–T338. https://doi.org/10.1190/geo2015-0399.1

Converse A, Brady AG (1992) *BAP basic strong-motion accelerogram processing software version 1.0*

Dobry R, Borcherdt RD, Crouse CB, et al. (2000) New Site Coefficients and Site Classification System Used in Recent Building Seismic Code Provisions. *Earthquake Spectra* 16:41–67

Far H, Fatahi B, Samali B (2012) Effects of soil dynamic properties and bedrock depth on seismic response of building frames incorporation soil-structure interaction. *In: Proc. 5th Asia-Pacific Conference on Unsaturated Soils*. pp 504 – 510

Field EH, Jacob KH (1995) A comparison and test of various site response estimation techniques, including three that are non reference- site dependent. *Bull Seism Soc Am* 86:991–1005

Kagami H, Duke CM, Liang GC, Ohta Y (1982) Observation of 1- to 5-second microtremors and their application to earthquake engineering. Part II. Evaluation of site effect upon seismic wave amplification due to extremely deep soil deposits. *Bull Seism Soc Am* 72:987–998

Konno K, Ohmachi T (1998) Ground-motion characteristics estimated from spectral ratio between horizontal and vertical components of microtremor. *Bull Seism Soc Am* 88:228–241

Kottke AR, Wang X, Rathje EM (2013) *Technical manual of STRATA*

Kramer SL (1996) *Geotechnical Earthquake Engineering*. Prentice Hall, Englewood Cliffs, New Jersey, USA

Langston CA (1979) Structure under Mount Rainier, Washington, inferred from teleseismic body waves. *J Geophys Res* 84:4749–4762

Liu HP, Warrick RE, Westerlund RE, et al. (1992) Observation of local site effects at a downhole – and – surface station in the Marina district of San Fransisco. *Bull Seism Soc Am* 82:1563–1591

MacMurdo J (1824) Papers relating to the earthquake which occurred in India in 1819. *Philosophical Magazine* 63:105–177

Manandhar S, Cho HI, Kim DS (2016) Effect of Bedrock Stiffness and Thickness of Weathered Rock on Response Spectrum in Korea. *KSCE Journal of Civil Engineering* 20.

Nakamura Y (1989) A method for dynamic characteristics estimation of subsurface using microtremor on the ground surface. *Quarterly Report of the Railway Technical Reasearch Institute* 30:25–33

Nogoshi M, Igarashi T (1970) On the propagation characteristics of microtremors. *J Seism Soc Japan* 23:264–280

Pandey B, Jakka RS, Kumar A, Mittal H (2016) Site Characterization of Strong-Motion Recording Stations of Delhi Using Joint Inversion of Phase Velocity Dispersion and H/V Curve. *Bull Seism Soc Am* 106:1254–1266. https://doi.org/10.1785/0120150135

Pandey B, Jakka RS, Kumar A, Sharma ML (2021) Site characterization of strong-motion stations of Himalaya and adjoining plains. *Arabian Journal of Geosciences* 14, https://doi.org/10.1007/s12517-021-07231-y

Parolai S, Bindi D, Augliera P (2000) Application of the Generalized Inversion Technique (GIT) to a microzonation study: numerical simulations and comparison with different site-estimation techniques. *Bull Seism Soc Am* 90:286–297

Parolai S, Bindi D, Troiani L (2001) Site response for the RSM seismic network and source parameters in the Central Apennines Italy. *Pure Appl Geophys* 158:695–715

Parolai S, Richwalski SM, Milkereit C, Bormann P (2004) Assessment of the stability of H/V spectral ratio from ambient noise and comparison with earthquake data in the Cologne area Germany. *Tectonophysics* 390:57–73

Pitilakis K (2004) Site Effects. *In: Ansal A (ed) Recent Advances in Earthquake Geotechnical Engineering and Microzonation*. pp 139–197

Riepl J, Bard PY, Hatzfeld D, et al. (1998) Detailed evaluation of site response estimation methods across and along the sedimentary valley of Volvi (EURO-SEISTEST). *Bull Seism Soc Am* 88:488–502

Rodriguez-Marek A, Bray JD, Abrahamson NA (2001) An empirical geotechnical seismic site response procedure. *Earthquake Spectra* 17:65–87

Safak E (2001) Local site effects and dynamic soil behavior. *Soil Dynamics and Earthquake Engineering* 21:453–458

Schnabel PB (1973) *Effects of local geology and distance from source on earthquake ground motion.* University of California

737 Seed HB, Idriss IM (1970) Soil moduli and damping factors for dynamic response analysis.
738 Berkeley
739 Seed HB, Wong RT, Idriss IM, Tokimatsu K (1986) Moduli and damping factors for dynamic
740 analysis of cohesionless soils. *Journal of Geotechnical* 112:1016–1032
741 Steidl JH, Tumarkin AG, Archuleta R (1996) What is a reference site? *Bull Seism Soc Am*
742 86:1733–1748
743 Triantafyllidis P, Hatzidimitriou PM, Theodulidis M, et al. (1999) Site effects in the city of
744 Thessaloniki (Greece) estimated from acceleration data and 1D local soil profiles. *Bull*
745 *Seism Soc Am* 89:521– 537
746

747 # 8. Tables

748 *Table 1: Details of Indian sites belonging to different groups as per their V_{S30} and depth of*
749 *engineering bedrock*(Pandey et al. 2021).

S. No.	Station	$V_{S,30}$ (m/s)	D_{EB} (m)	$V_{S,HS}$ (m/s)	D_{HS} (m)	Group/Figure
1	IGNOU	493	40	1600	345	G1a Figure 2 - 5
2	IMD	543	40	1250	120	
3	JNU	565	22	1400	97	
4	ANDC	564	32	2000	342	
5	DJB	543	16	2500	916	
6	VCD	550	22	1800	106	
7	MUN	582	35	1400	165	
8	CHP	459	41	1800	300	
9	PATI	497	32	1500	240	
10	PTH	551	22	1250	142	
11	BAG	736	9	2200	148	
12	KAP	440	45	1050	45	
13	RNKT	554	20	2700	637	
14	NTL	412	43	1175	193	
15	THRI	473	25	1600	275	
16	DNLT	418	41	1800	253	
17	RDPR	676	9	2300	348	
18	JMTH	522	24	1650	217	
19	PAU	577	12	1700	114	
20	LNSD	540	25	1600	190	
21	DMKT	577	22	2200	354	
22	UTKS	564	24	2200	564	
23	CKT	622	21	2100	141	
24	TNKP	426	45	1600	509	
25	VKN	475	40	1400	445	

26	NSIT	391	80	1700	596	G1b Figure 6
27	BKT	393	55	925	55	
28	IGIV	360	133	1700	438	G1c Figure 7
29	KOT	497	112	1200	272	
30	MBD	365	110	1025	265	
31	DU	345	65	1375	150	G2b Figure 8
32	IPU	328	94	1200	269	
33	ZHC	337	67	950	67	
34	NPTI	322	76	1200	196	
35	GOPE	345	79	1100	175	
36	HW	357	95	1000	185	
37	GEC	338	178	1100	603	G2c Figure 9 - 11
38	SCRG	346	122	1750	547	
39	DTU	323	115	1250	575	
40	KSPR	282	154	875	304	
41	USN	244	-	750	315	
42	KTM	338	145	900	205	
43	RK	267	-	750	255	
44	SMBL	338	120	950	345	
45	NOIDA	249	392	775	249	
46	NJBD	207	-	625	114	
47	MEE	327	200	900	200	
48	GHZ	320	156	1000	356	
49	DEO	312	264	800	264	
50	CHND	312	172	950	387	
51	BIJ	298	-	750	208	
52	BRT	309	154	825	294	
53	ANUP	350	162	1025	392	
54	RMPR	277	-	750	169	
55	PILI	262	167	1000	507	
56	NKR	309	166	1000	476	
57	MZNR	271	256	760	256	
58	BHR	257	-	700	145	
59	KHTL	271	-	750	214	
60	SHNP	341	177	900	257	
61	BLND	325	217	875	267	
62	GARH	321	218	850	218	

752 *Table 2: Details of Kik-Net sites belonging to different groups as per their V_{S30} and depth of*
753 *engineering bedrock.*

S. No.	Station	$V_{S,30}$ (m/s)	D_{EB} (m)	$V_{S,HS}$ (m/s)	D_{HS} (m)	Group/Figure
1	AOMH05	238	26	1210	294	G2a Figure 12
2	AOMH09	261	26	1720	136	
3	KKWH11	242	48	1600	76	
4	KKWH13	355	24	1400	120	
5	FKIH04	300	80	2300	98	G2b Figure 13
6	MYGH05	305	86	1080	260	
7	NMRH02	315	94	870	94	
8	AICH23	202	160	1600	760	G2c Figure 14
9	KNGH22	339	175	2120	800	

754

755 Table 3: Summary of results and corresponding recommendations for different cases.

S.No.	$V_{S,30}$ (m/s)	NEHRP Site Class	Sub-Site Class	f_0	Recommended V_S for Bedrock (m/s)
1	600 & more	C	C1	-	2000
2	500 to 600		C2	≥ 5Hz	1500
3	< 500		C3	>3Hz	1200
4			C4	~1Hz	>1500
5	> 300	D	D1	≥2Hz	1000
6			D2	~1Hz or lesser	>1200
7	240 - 300		D3	-	>800
8	< 240		D4	-	EB/major impedance contrast due to stiff soil or soft/hard rock

756

9. Figures

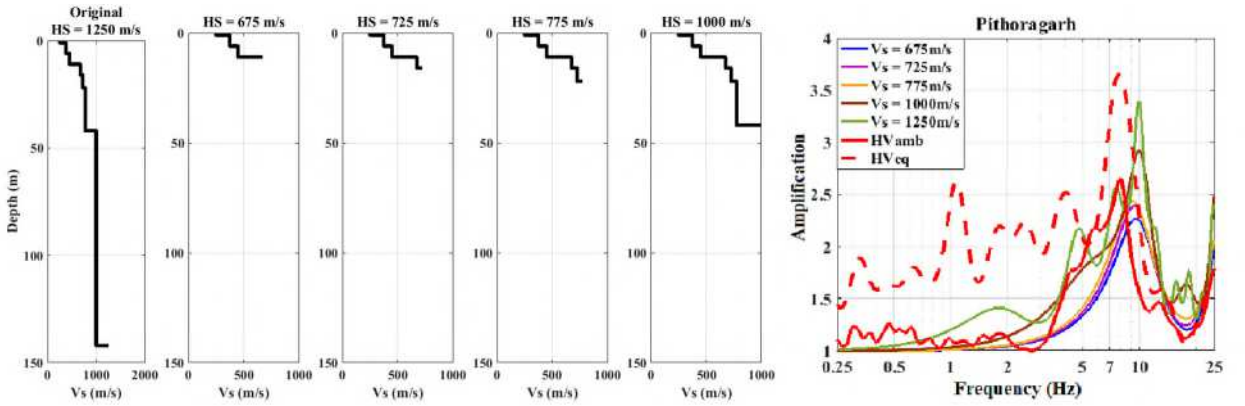

Figure 1: Typical example of different V_S models used to study the effect of bedrock depth for a site (Pithoragarh in this case) and transfer functions obtained.

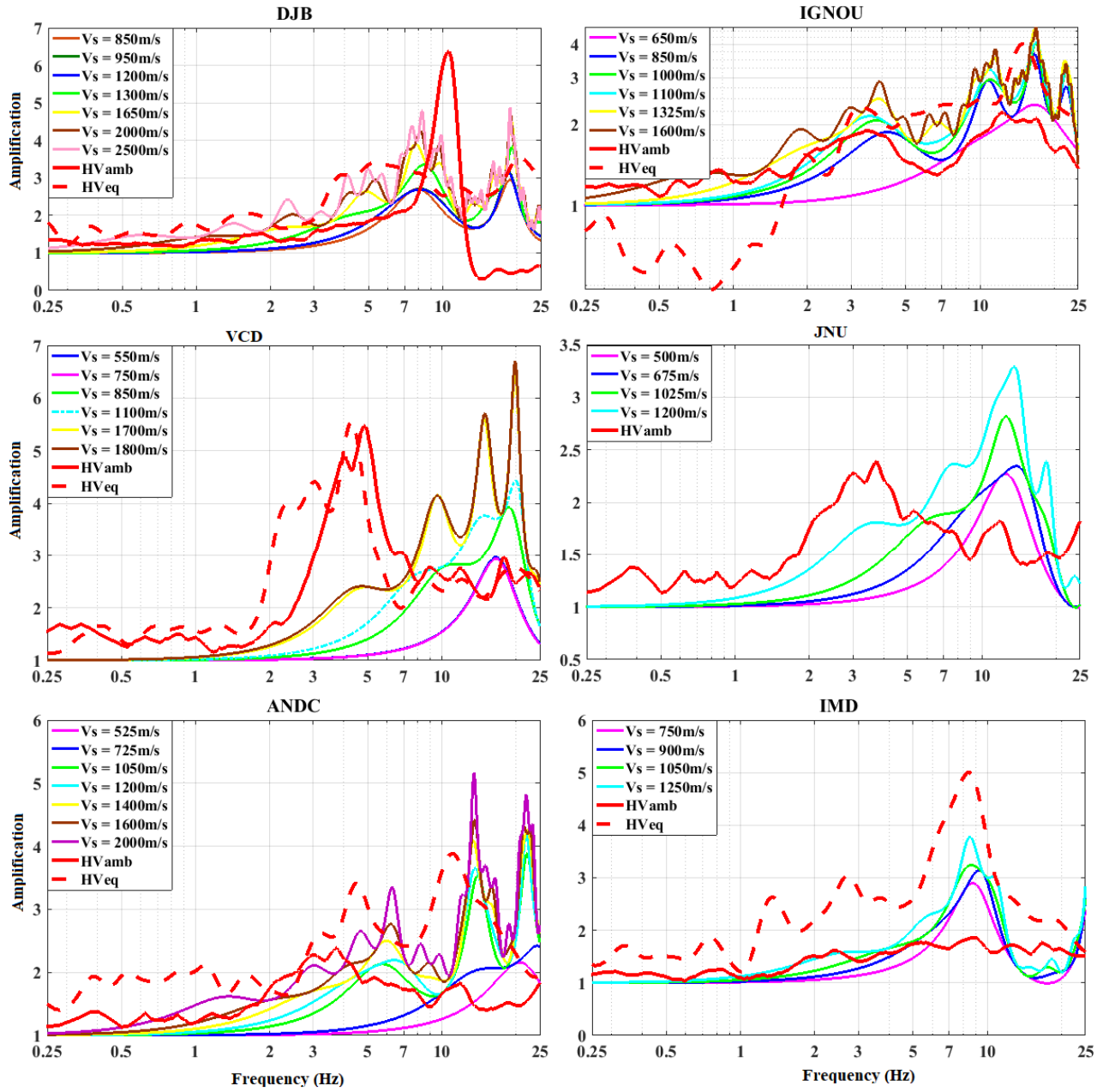

Figure 2: Comparison of TF between the surface and internal layer, having high Vs, as outcrop (reference site) with HVSR from ambient noise and earthquake records for G1a sites of Delhi

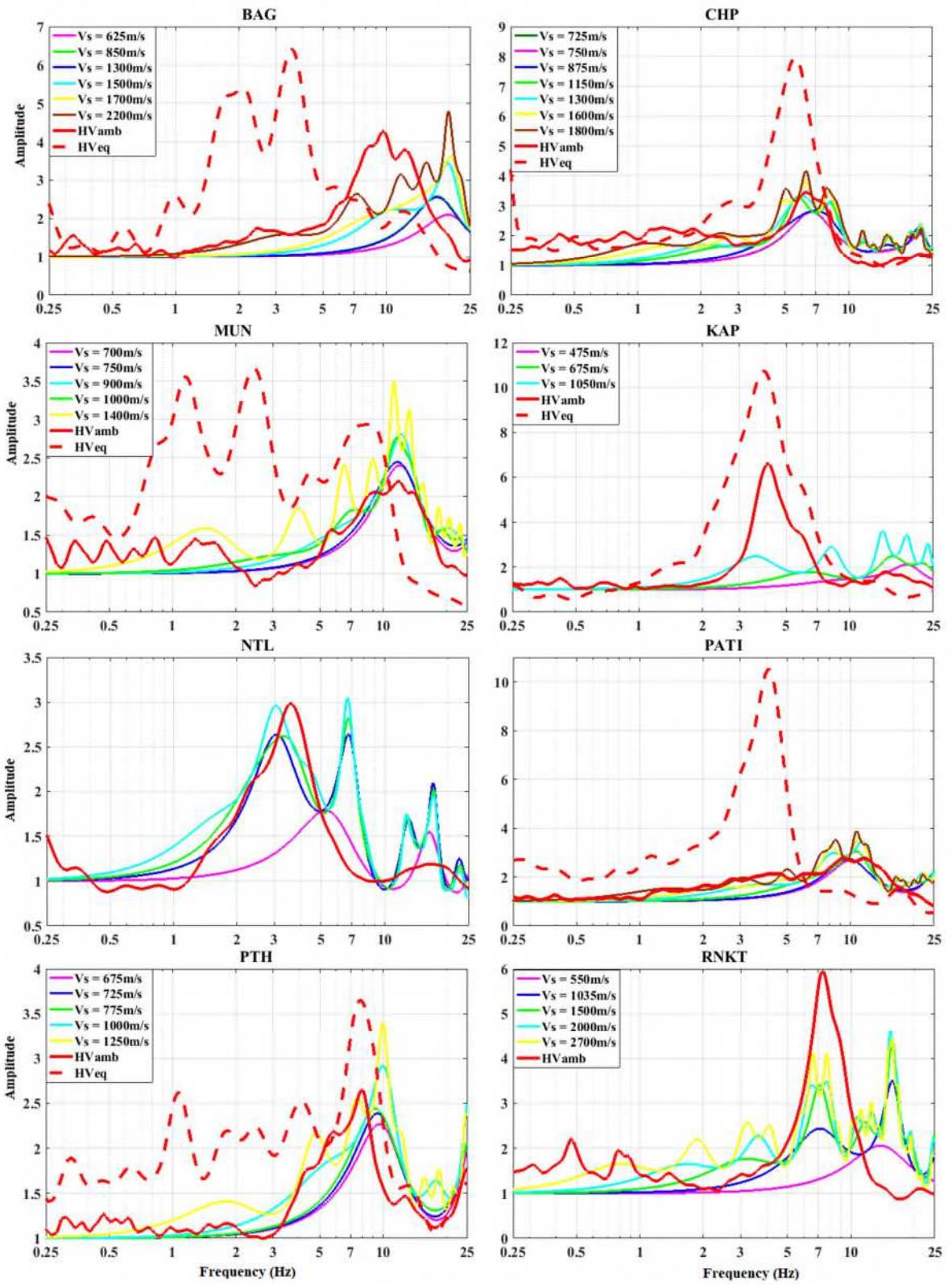

Figure 3: Comparison of TF between the surface and an internal layer having high Vs, as outcrop (reference site) with HVSR from ambient noise and earthquake records for G1a sites of Kumaun

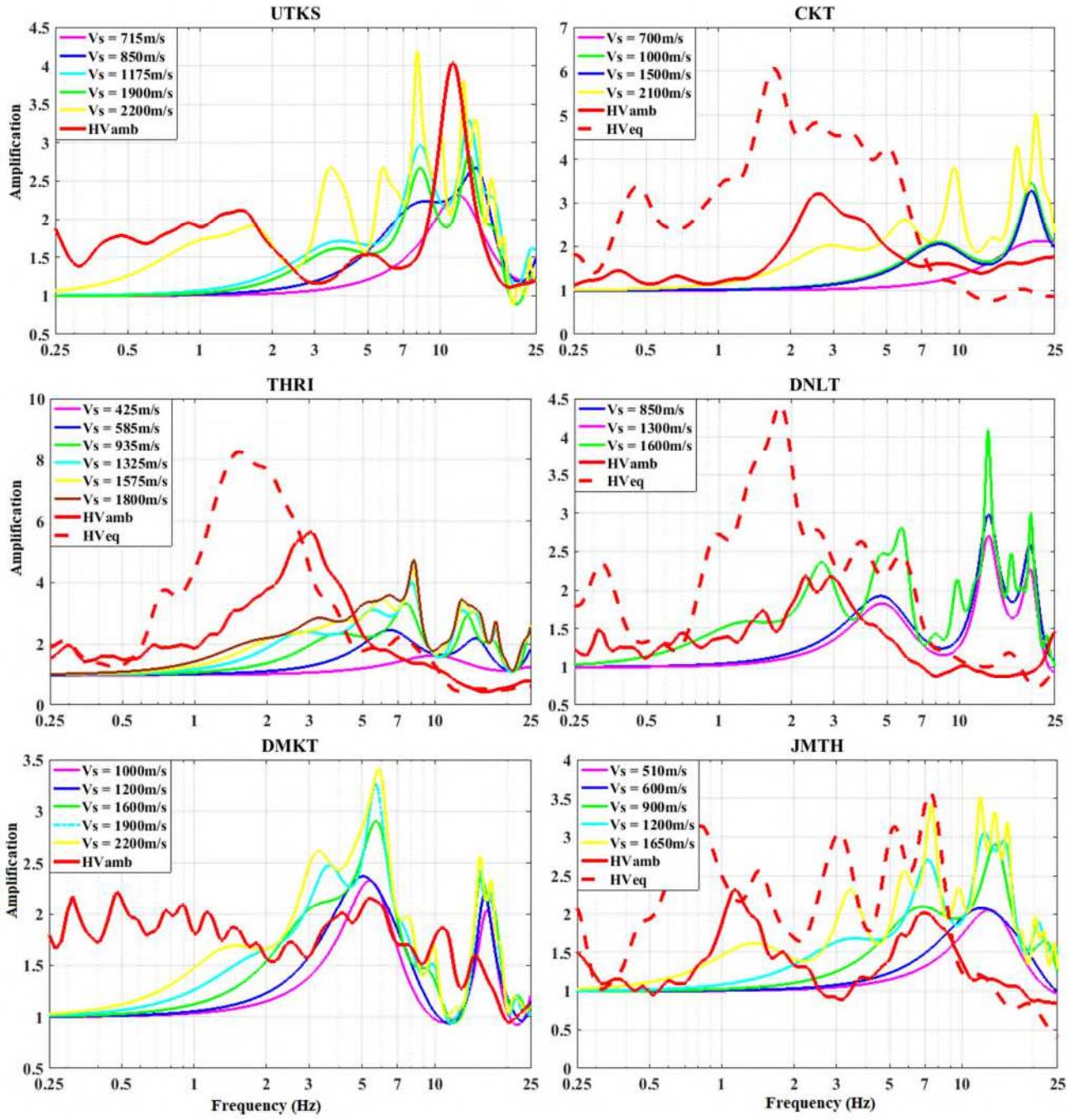

Figure 3: Comparison of TF between the surface and internal layer having high Vs, as outcrop (reference site) with HVSR from ambient noise and earthquake records for G1a sites of Garhwal

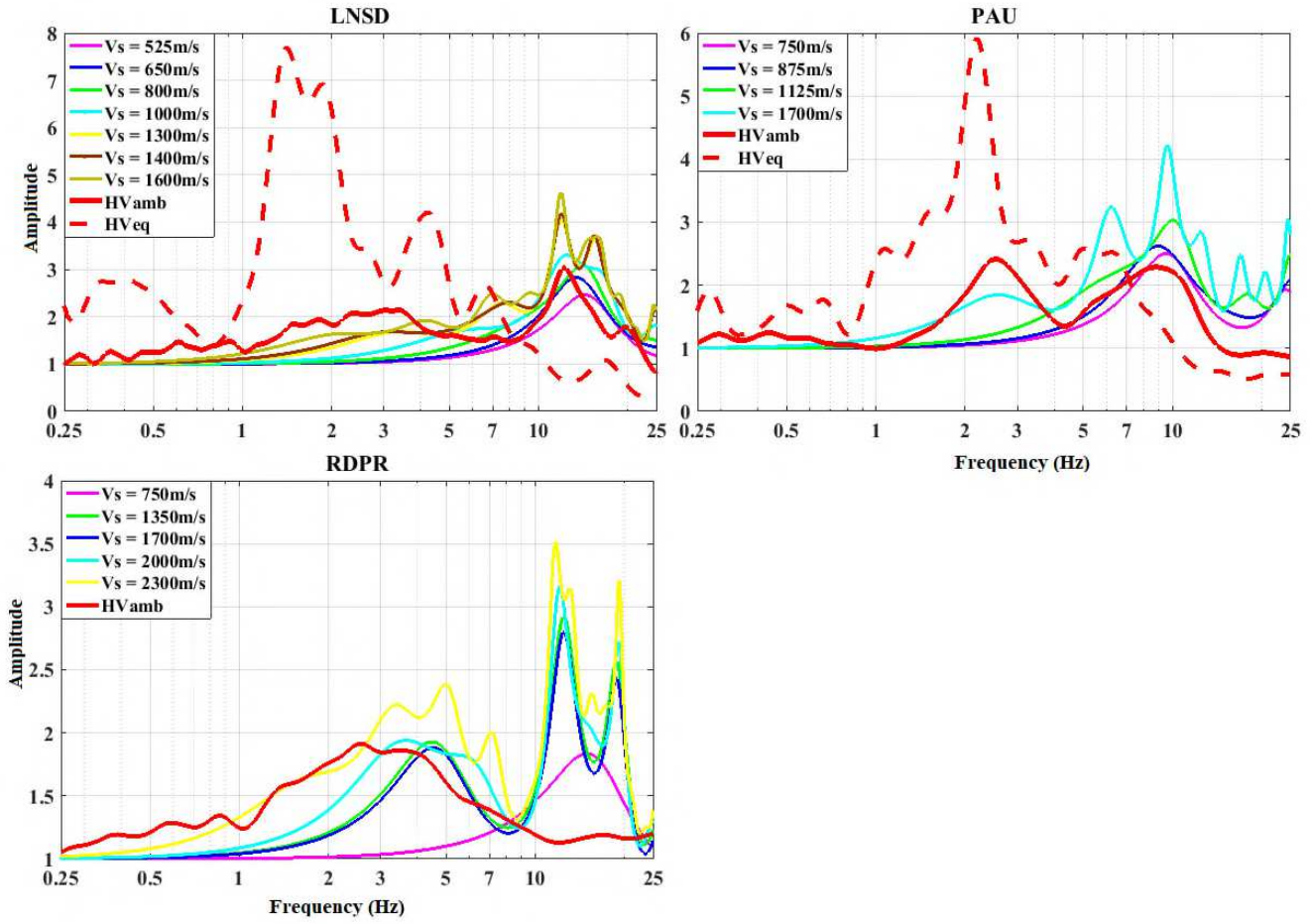

Figure 0 (Continued): Comparison of TF between the surface and internal layer having high Vs, as outcrop (reference site) with HVSR from ambient noise and earthquake records for G1a sites of Garhwal

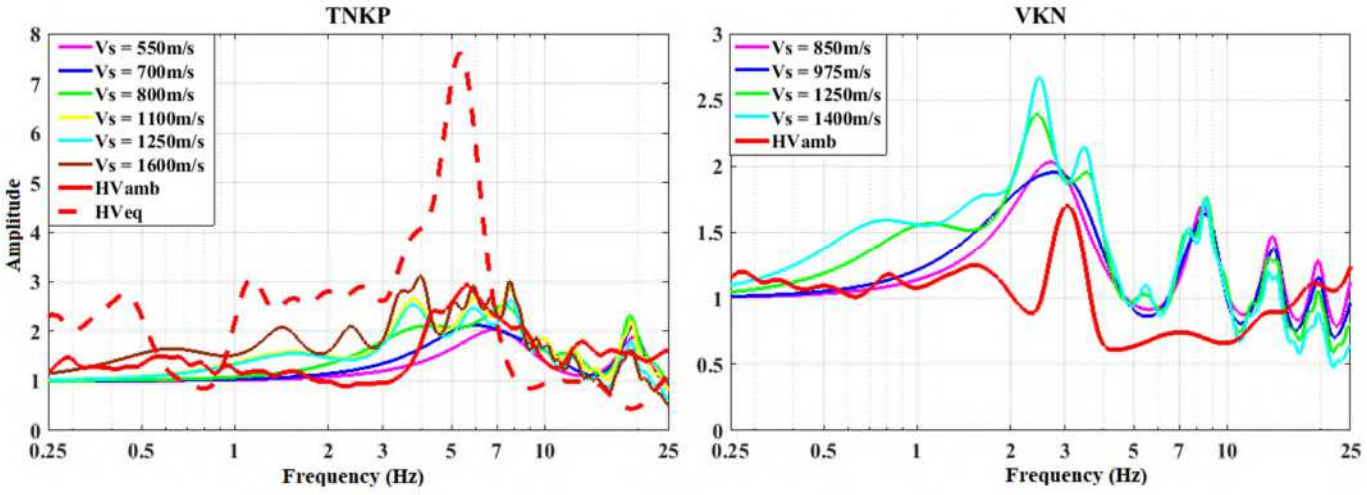

Figure 5: Comparison of TF between the surface and internal layer having high Vs, as outcrop (reference site) with HVSR from ambient noise and earthquake records for G1a sites of Tarai

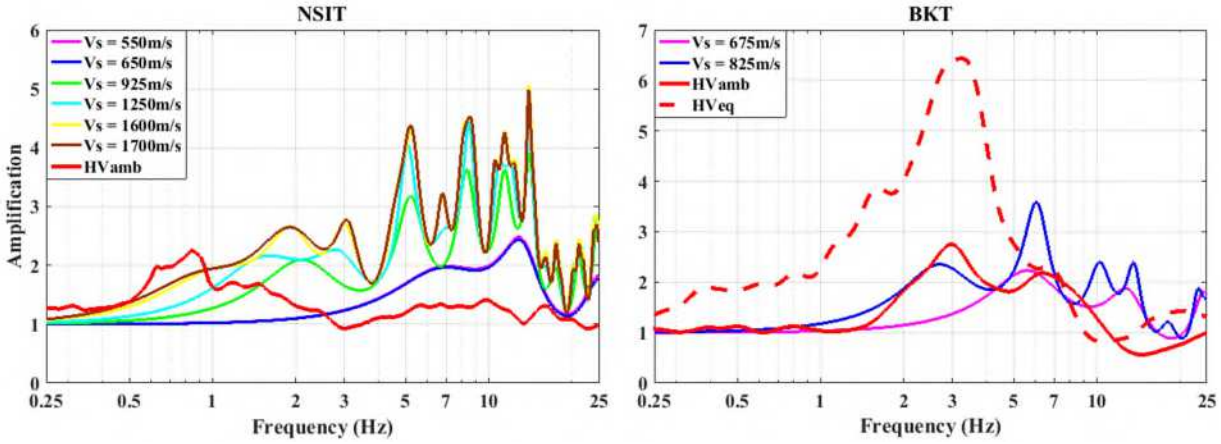

Figure 6: Comparison of TF between the surface and internal layer having high Vs, as outcrop (reference site) with HVSR from ambient noise and earthquake records for G1b sites

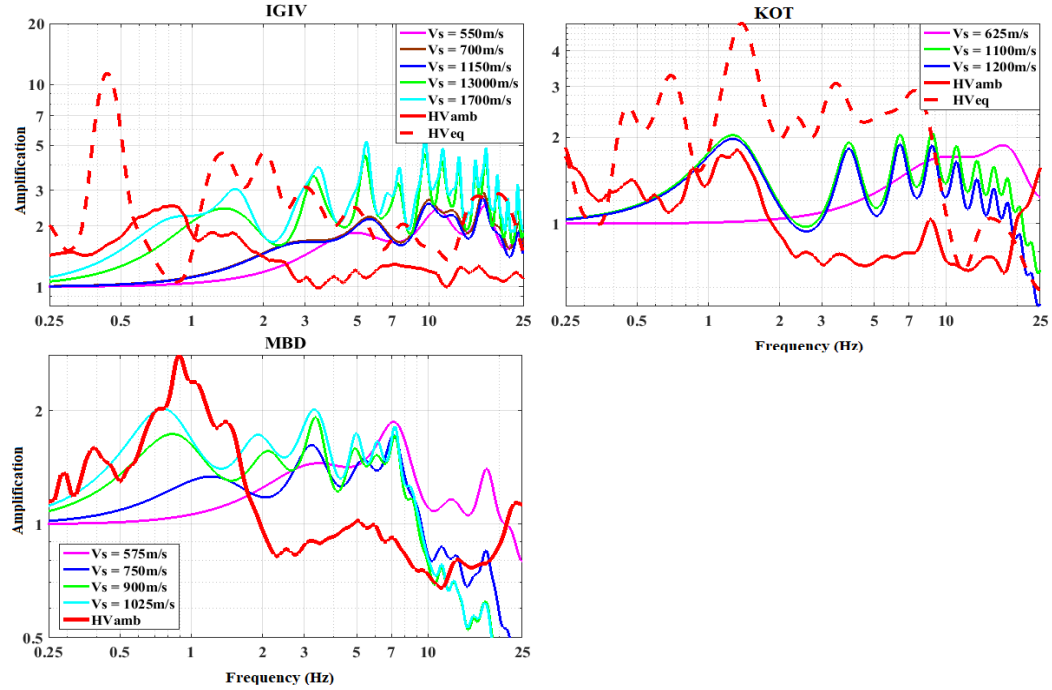

Figure 6: Comparison of TF between the surface and internal layer having high Vs, as outcrop (reference site) with HVSR from ambient noise and earthquake records for G1c sites

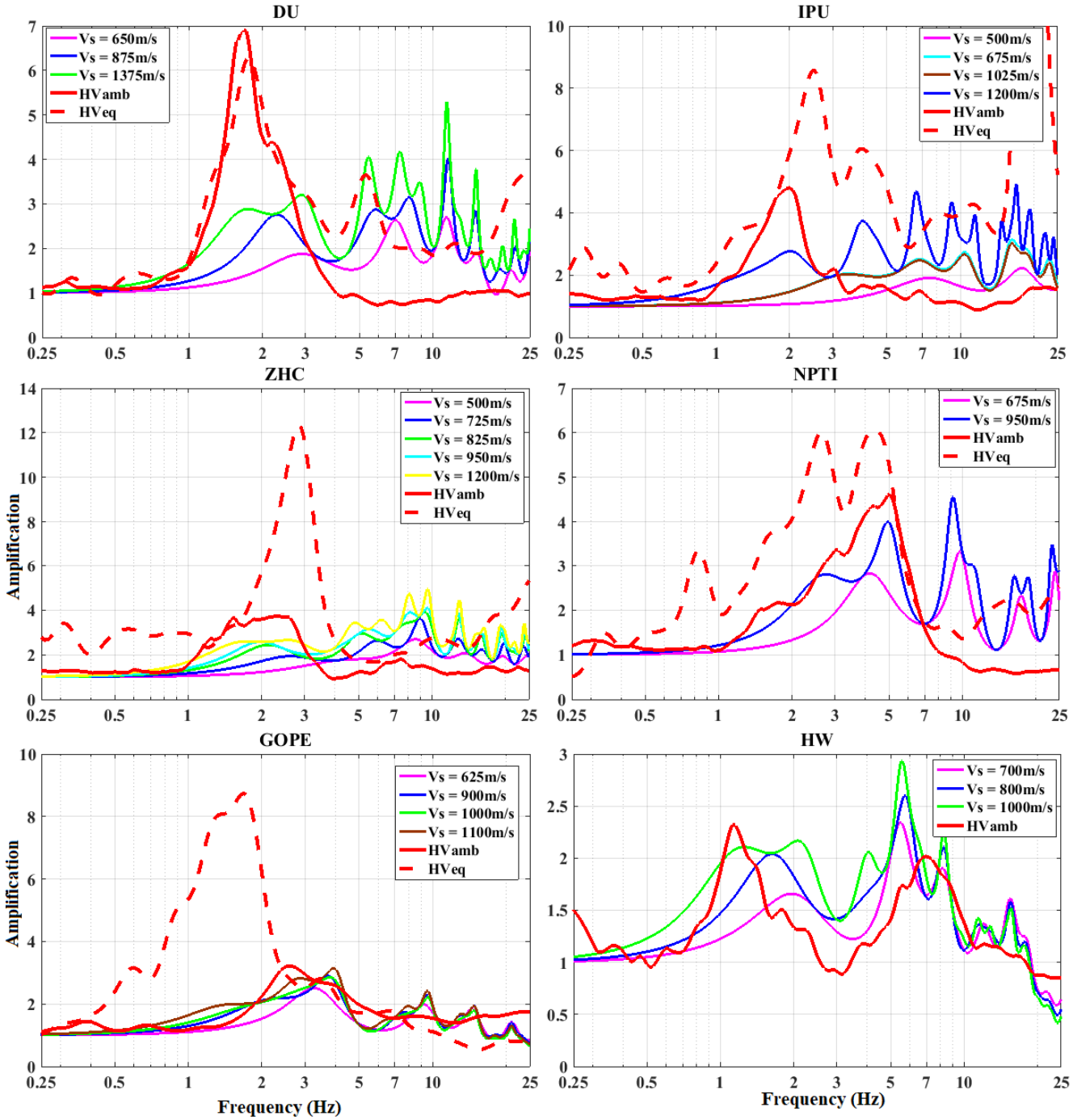

Figure 7: Comparison of TF between the surface and internal layer, having high Vs, as outcrop (reference site) with HVSR from ambient noise and earthquake records for G2b sites.

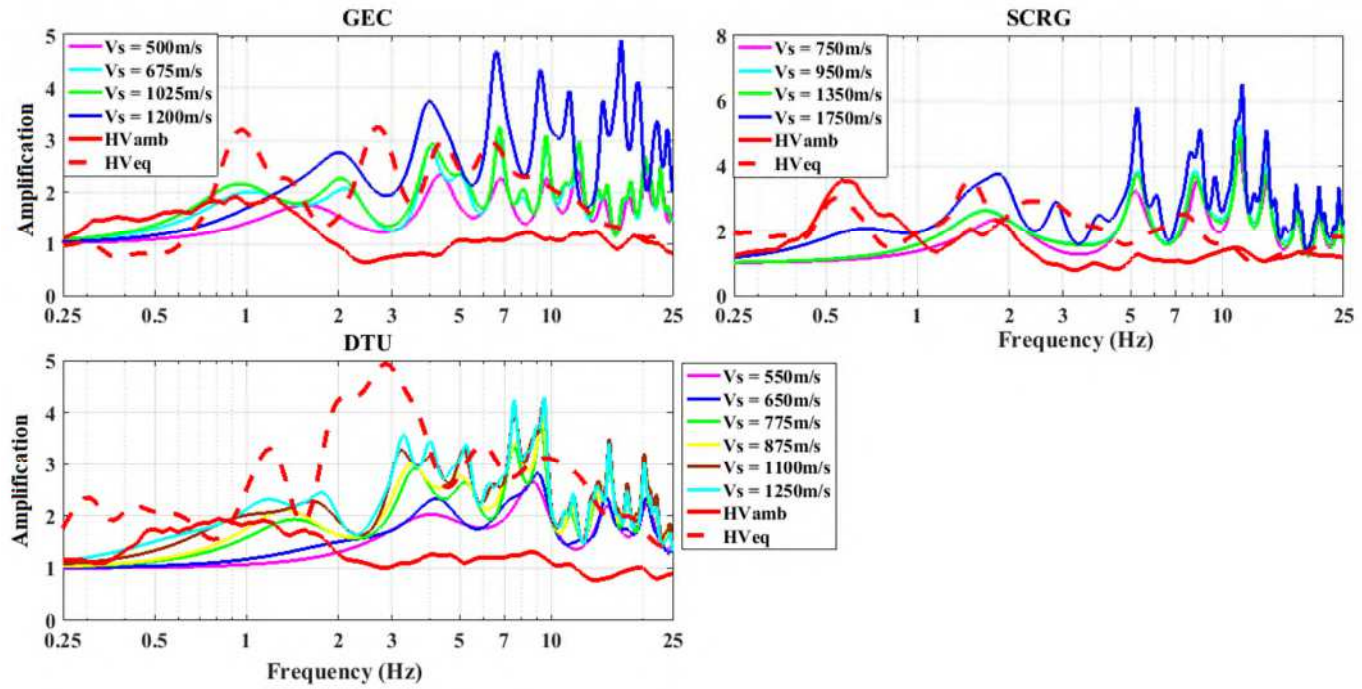

Figure 8: Comparison of TF between the surface and internal layer, having high Vs, as outcrop (reference site) with HVSR from ambient noise and earthquake records for G2c sites Delhi.

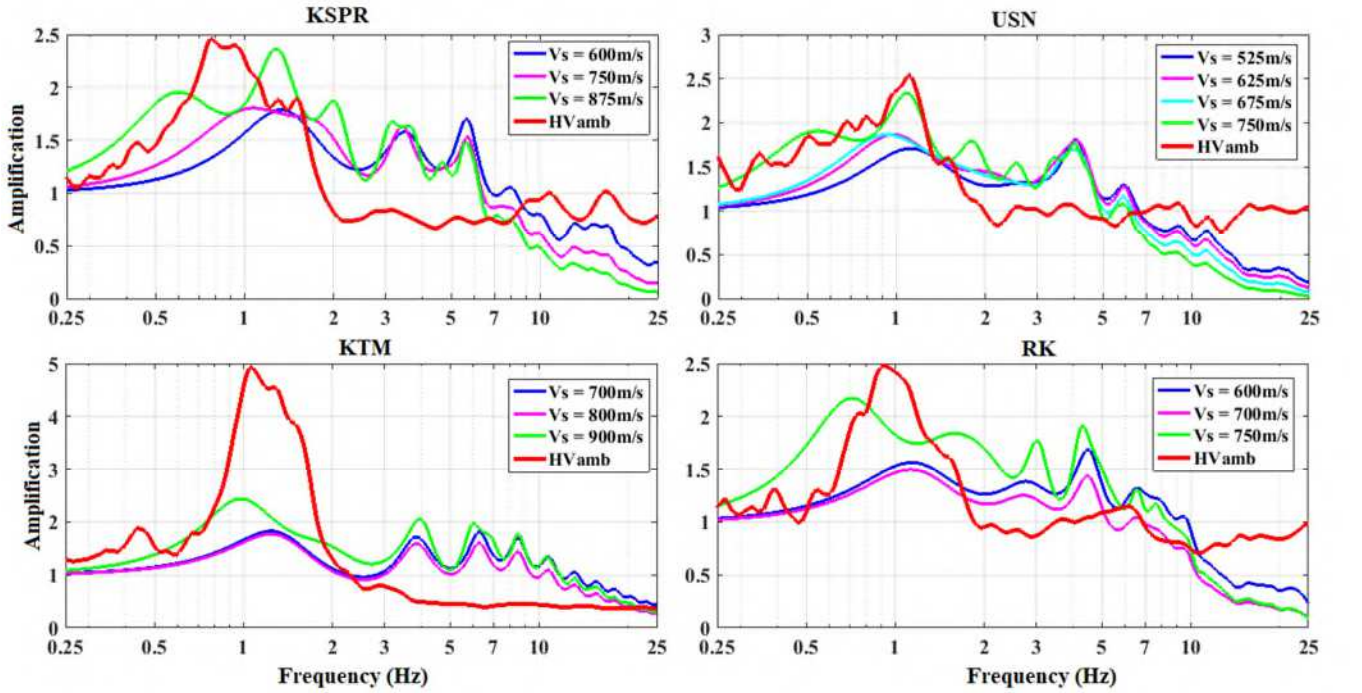

Figure 9: Comparison of TF between the surface and internal layer, having high Vs, as outcrop (reference site) with HVSR from ambient noise and earthquake records for G2c sites of Tarai.

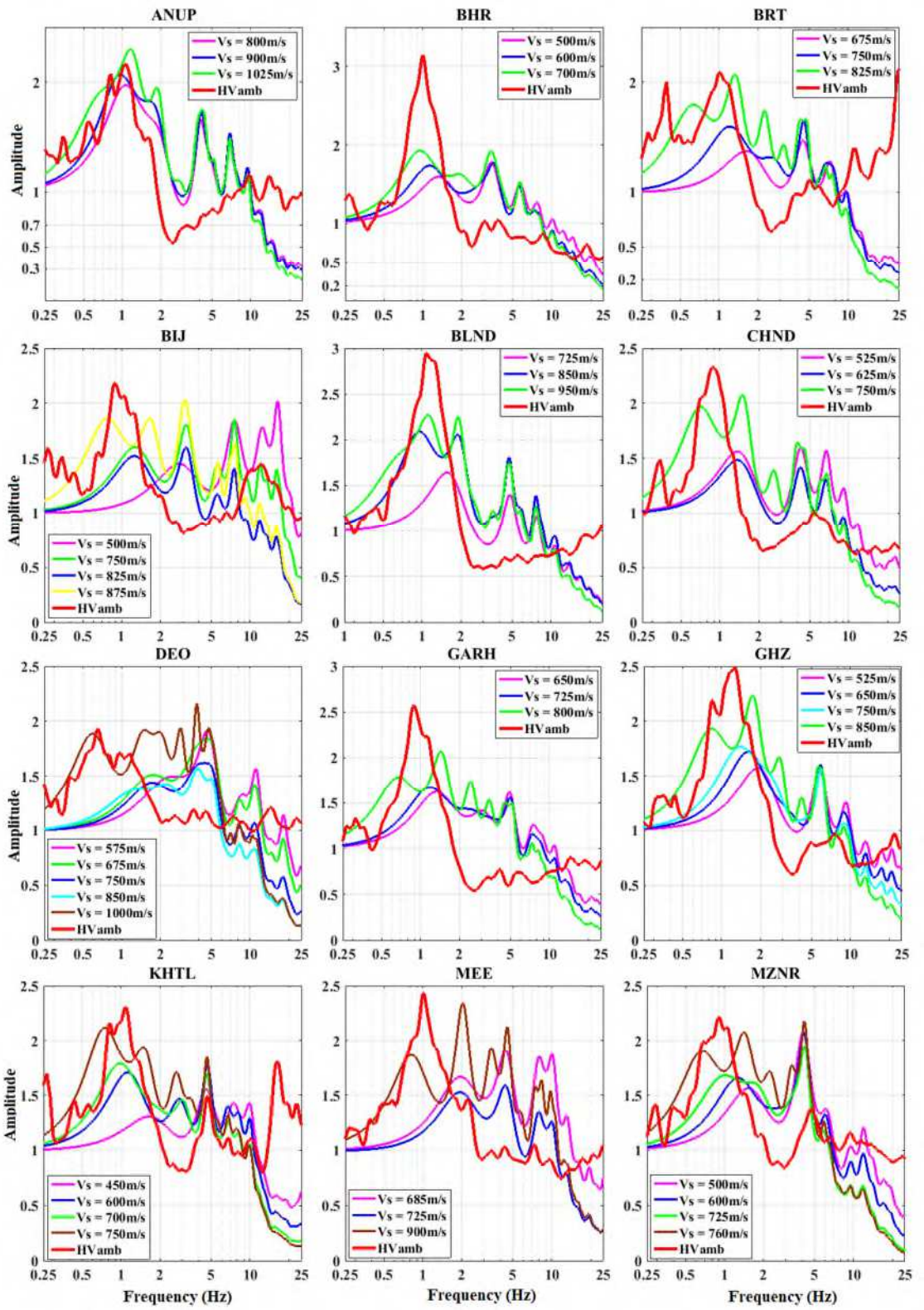

Figure 10: Comparison of TF between the surface and internal layer, having high Vs, as outcrop (reference site) with HVSR from ambient noise and earthquake records for G2c sites of Western UP

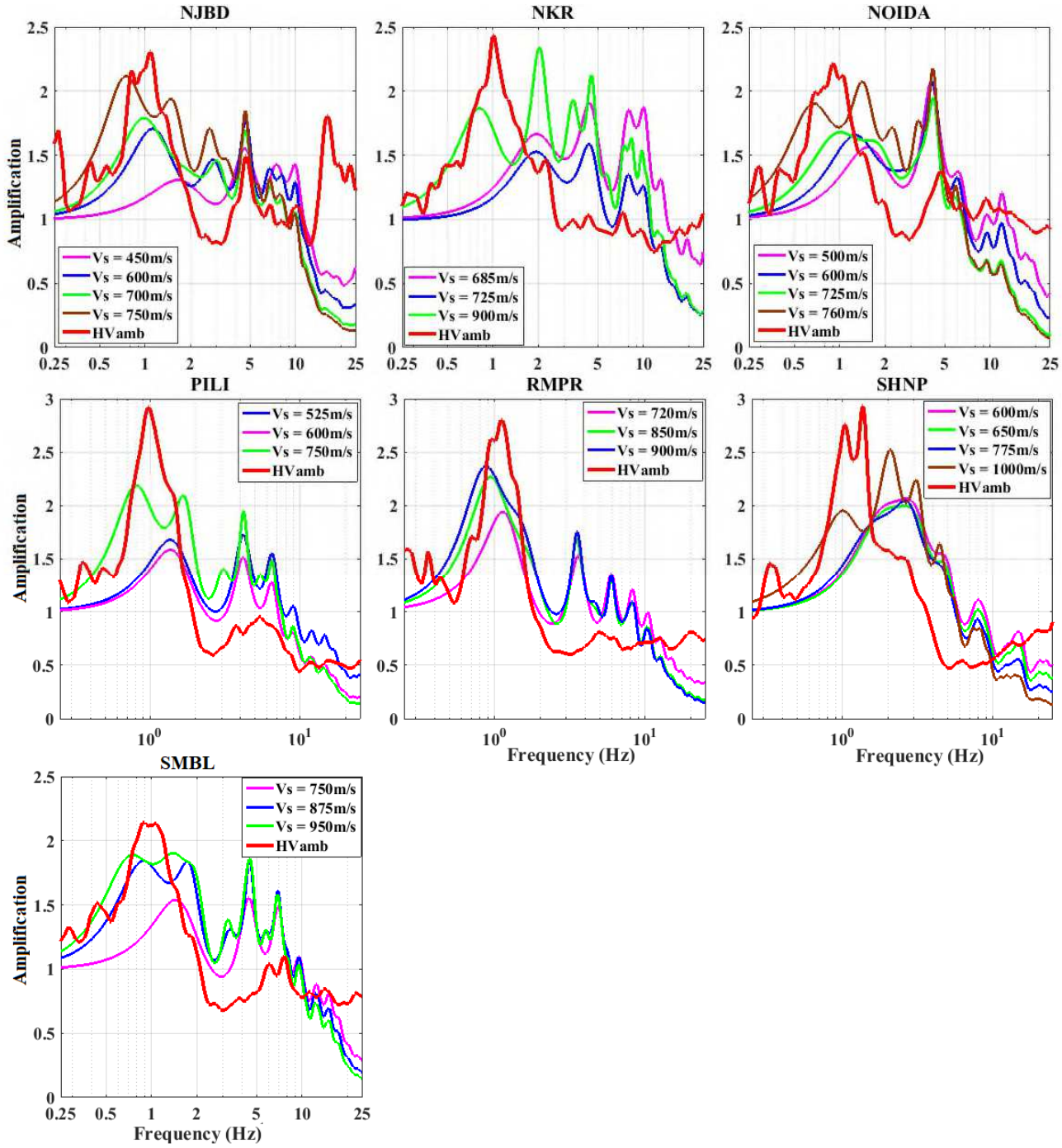

Figure 11 (Continued): Comparison of TF between the surface and internal layer, having high Vs, as outcrop (reference site) with HVSR from ambient noise and earthquake records for G2c sites of Western UP

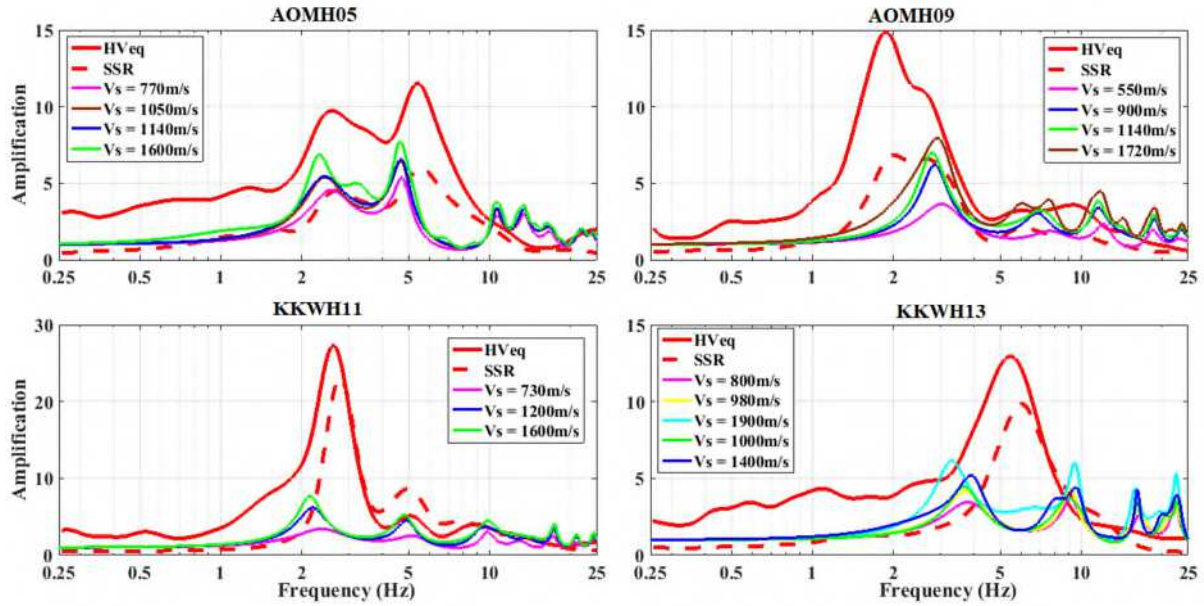

Figure 12: Comparison of TF between the surface and internal layer from GRA, having high Vs, as outcrop (reference site) with SSR and HV_{eq} for G2a sites from Kik-Net database

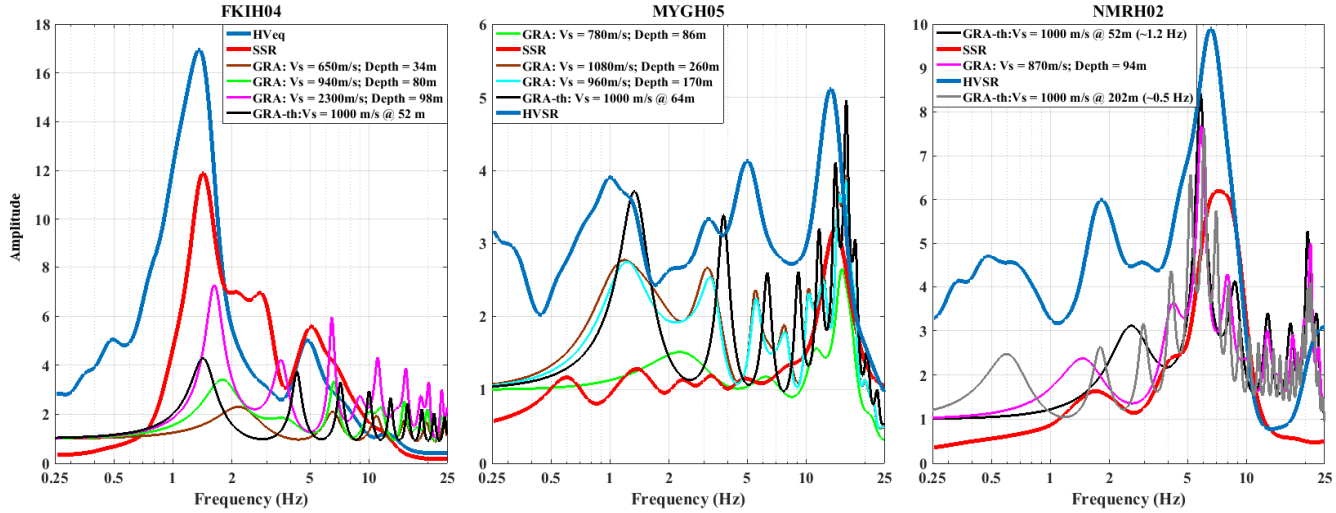

Figure 13: Comparison of TF between the surface and internal layer from GRA, having high Vs, as outcrop (reference site) with SSR and HV_{eq} for G2b sites from Kik-Net database

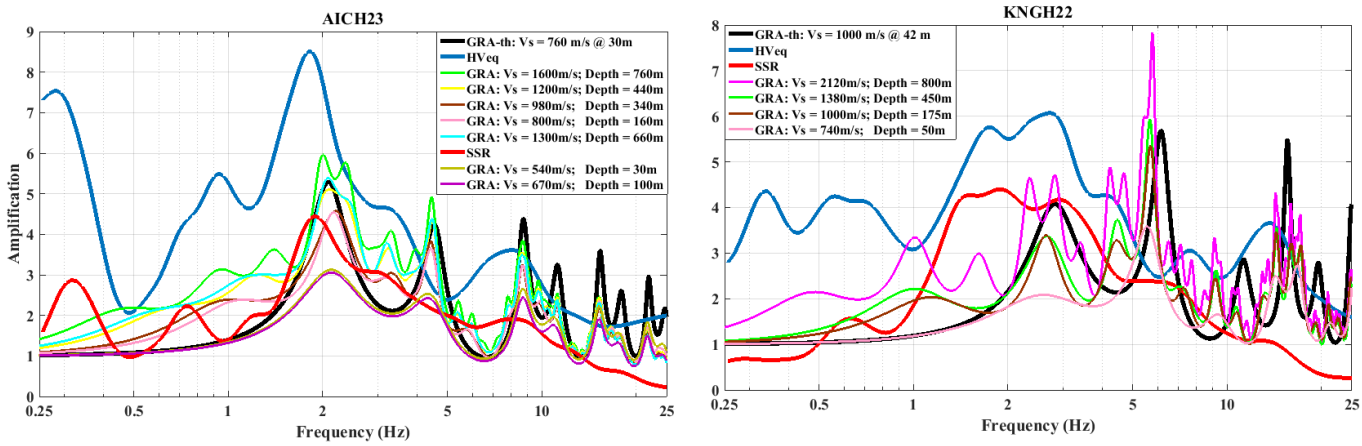

Figure 14: Comparison of TF between the surface and internal layer from GRA, having high Vs, as outcrop (reference site) with SSR and HV_{eq} for G2c sites from Kik-Net database.